

Otay Mesa, California, Tunnel Search Mission, 28 Jan 2003 Seismic Search for Underground Anomalies

Rick Miller
Julian Ivanov
Choon Park
David Laflen
Jason Blair

Kansas Geological Survey
1930 Constant Avenue
Lawrence, Kansas 66047

Final Report to

Jose Llopis
U.S. Army Corps of Engineers
Vicksburg, Mississippi

Open-file Report #2003-61

March 2003

After Action Review
Otay Mesa, California, Tunnel Search Mission
28 Jan 2003

Seismic Search For Underground Anomalies
Rick Miller, Julian Ivanov, and Choon Park
Kansas Geological Survey
University of Kansas
Lawrence, Kansas

ISSUE

Unauthorized infiltration into the U.S. is possible through the air, from the sea, across the land, and under the ground. A variety of extremely efficient and effective detection and deterrent systems are available, in use, and/or under development that reasonably address illegal encroachment on U.S. territory through all these methods except from beneath the earth surface. Several near-surface geophysical techniques have been evaluated and in certain situations and with the appropriate set of assumptions show promise in detecting underground activity related to tunneling. Surface seismic—both passive and active—possess demonstrated potential, but lack efficiency in operation and high confidence, independent identification techniques. Recently developed acquisition and analysis techniques for multichannel surface wave imaging has opened the door to a vast number of near-surface applications including anomaly detection and delineation, specifically tunnels.

High-resolution seismic techniques were used to search for anomalies in the first 100 ft below the ground surface at three California sites along the U.S./Mexico border (Figure 1). Anomalies that possessed seismic characteristics that appear consistent with those of a tunnel intended to illegally transport people and materials into the U.S. previously discovered in this area were the target of this study. Based on intelligence and a recent discovery of a vertical, hand dug, 60 ft deep shaft located about 700 ft south of the U.S./Mexico border near the Otay Mesa, California, Port of Entry (POE), three survey lines were positioned parallel to and less than 750 feet from the border fence at one site. A second suspect site located near San Ysidro, California, was located based on intelligence and centered around a warehouse located less than 100 ft south of the border fence. Two seismic survey lines were deployed in such a way as to intersect any tunneling activity originating in the warehouse and with a northerly heading.

Evaluating the potential of this imaging technology and establishing the seismic characteristics for tunnels in this geologic and cultural setting requires acquisition, processing, and analysis of empirical data in areas both with confirmed tunnels and those suspected to have tunnels. A previously discovered tunnel a mile or so west of the suspected POE investigation site was used to establish tunnel signatures for this area. A feasibility study at a spot where the tunnel reaches 65 ft below ground surface identified a unique wave arrival pattern consistent with the known tunnel location and model studies. This finding meets the first objective of this study, which was to first determine if these deeper tunnels (65 ft) have the same readily distinguishable, unique signature, as was observed where the tunnel was only 35 ft deep. The second, and primary, objective of this mission was to determine if suspected tunnels exist at these deeper depths at the two nearby sites. A longer term goal of this and many other similar studies was to continue building toward the development of a system that could be deployed along the border and provide routine surveillance capabilities beneath access roads and trails running parallel to and in proximity of the U.S./Mexico border.

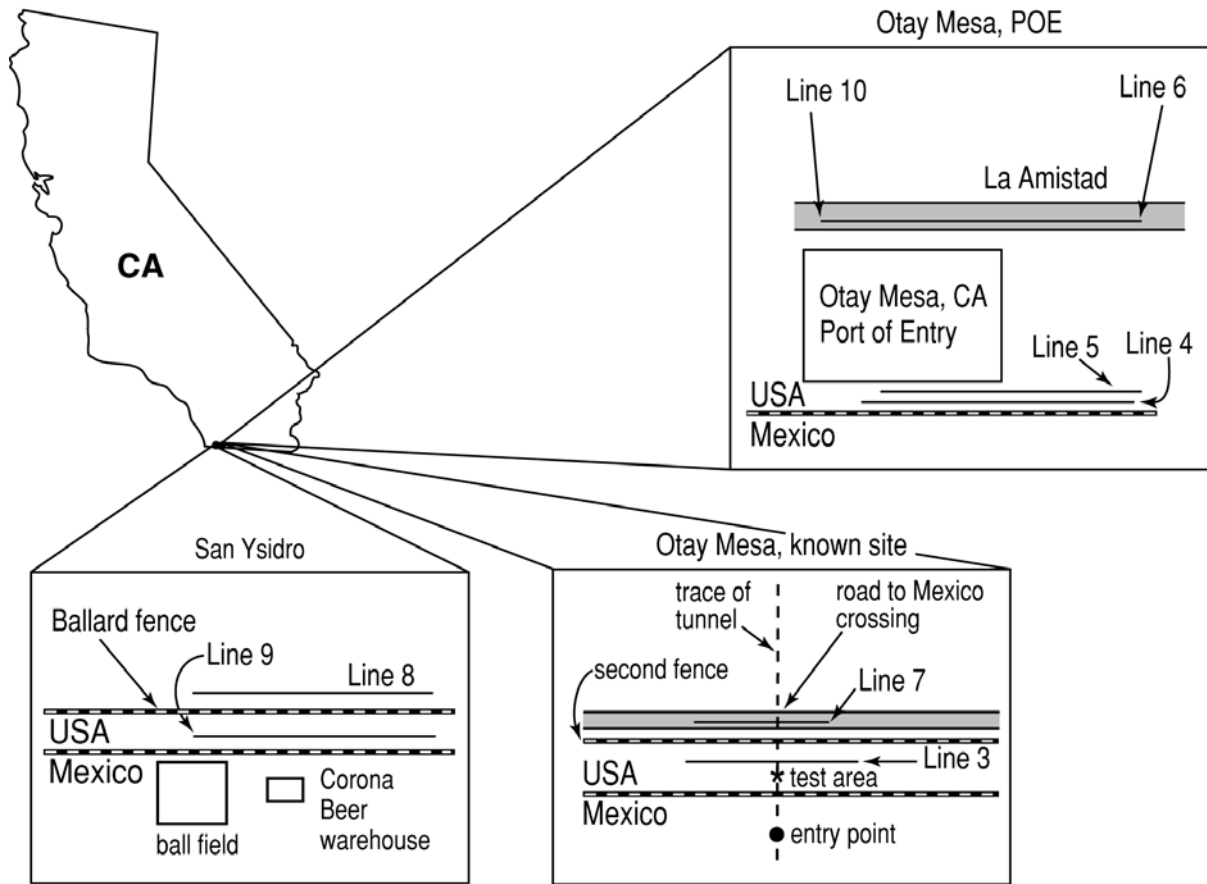


Figure 1. Site map with three individual search areas in general detail.

DISCUSSION

Historically, detection of anomalies using seismic methods has relied heavily on wavefield interference and point source radiation phenomena (Rechtien et al., 1995; Miller and Steeples, 1991; Steeples and Miller, 1988; Cook, 1965; Fisher 1971; Watkins et al., 1967). This approach can be effective in some situations, but considering the wealth of information contained in the wavefield, it is at best a cursory use of the information available in the wavefield. Recent development of surface seismic techniques designed to provide a quantitative measure of key seismic properties for each 3-D cell of a specified earth volume from a single shot gather by analyzing individual components of the wavefield has shown great promise (Miller et al., 2001). This project proved an incremental step in the evaluation of the potential of these seismic imaging and sampling techniques for shallow tunnel detection.

Ground truth was critical. Technique verification and fine tuning at the known tunnel site was essential for correlating between expected and observed variations in seismic properties interpreted to be indicative of possible targets. A tunnel known to exist at 65 ft below ground surface along the U.S./Mexico border near Otay Mesa, California, provided an excellent calibration target and site. Successfully capturing tunnel seismic signature of the 35 ft deep Otay Mesa tunnel was verified through model studies and ground truth correlations. Modeling and data analysis techniques developed on this project were based to a large degree on the empirical results of calibration studies over the location where the tunnel is known to be present, 65 ft below ground surface. Geologic or anthropogenic anomalies have been

successfully identified using various components of the wavefield and empirical correlations, some of these include: bedrock karst feature in southern Alabama and eastern Kansas (Miller and Xia, 1999; Miller et al., 1999) (Figure 2); faulted and/or mined out zones in southern Illinois (Figure 3); buried pipes at Lawrenceville, Illinois (Miller et al., 2000) (Figure 4), and San Jose, California (Figure 5); and a tunnel at 35 ft below ground surface at Otay Mesa, California (Miller et al., 2002) (Figure 6).

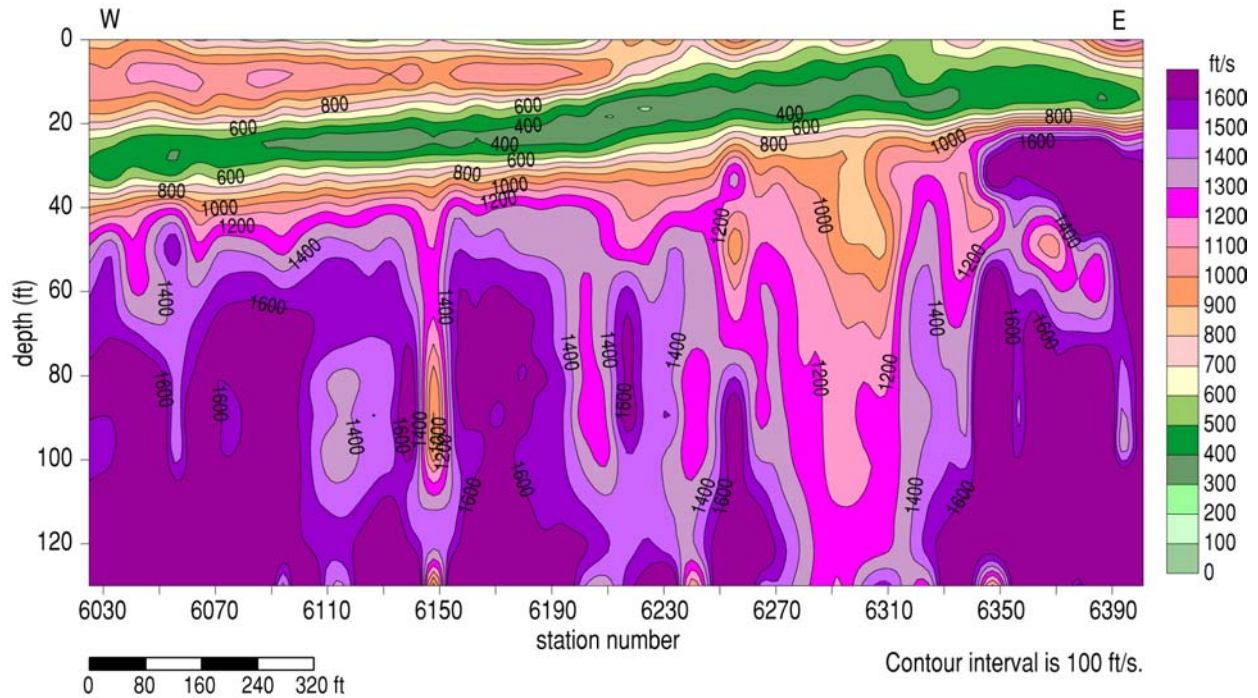


Figure 2. Shear-wave velocity contours. Dissolution features (karst) beneath undisturbed alluvial overburden were detected on shear wave velocity profiles at a proposed power plant site in Alabama.

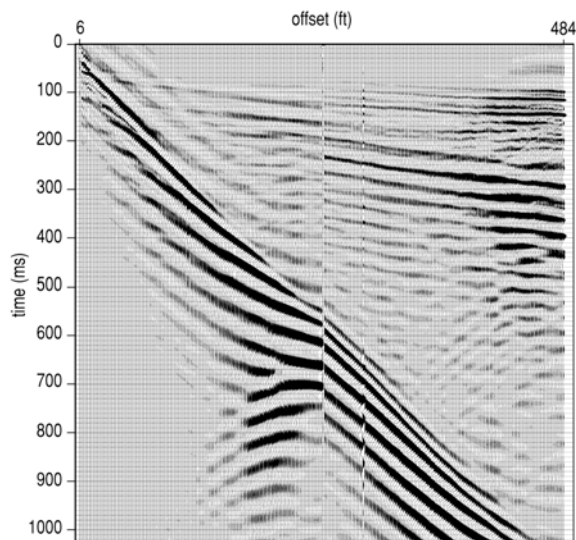


Figure 3. Walkaway shot gather of three sweeps from the shear wave vibrator vertically stacked. The scatter phenomena are easily interpreted on this seismogram.

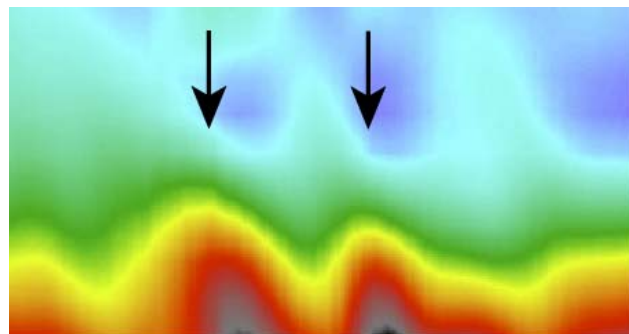


Figure 4. Phase and amplitude distortions in the 2-D shear wave velocity field at a refinery site in Illinois. Arrows indicate location of pipes.

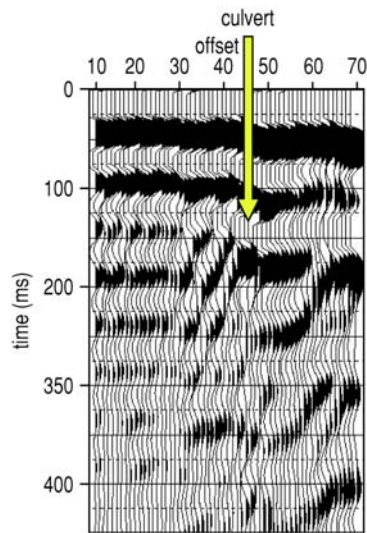


Figure 5. LMO stack with culvert location and associated scatter marked (near San Jose, California).

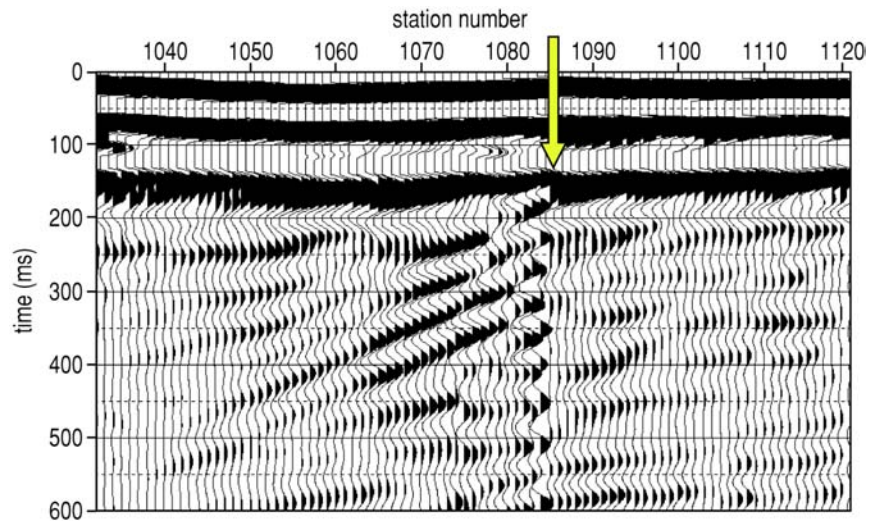


Figure 6. LMO stack with tunnel location indicated by arrow. Otay Mesa, California, tunnel at 35 ft below ground surface detected by anomalous reflected and diffracted backscatter at the tunnel location enhanced by processing.

Surface Wave Inversion and Wavefield Analysis

Surface waves traditionally have been viewed as noise on multichannel seismic data collected to image targets for shallow engineering, environmental, and ground water purposes (Steeple and Miller, 1990). Recent advances in the use of surface waves for near-surface imaging have combined spectral analysis techniques (SASW), developed for civil engineering applications (Nazarian et al., 1983), with multi-trace reflection technologies developed for near-surface (Schepers, 1975) and petroleum applications (Glover, 1959). The combination of these two uniquely different approaches to seismic imaging of the shallow subsurface permits non-invasive estimation of shear wave velocity and delineation of horizontal and vertical variations in near-surface material properties based on changes in these velocities (MASW) (Park et al., 1996; Xia et al., 1999; Park et al., 1999).

Extending this imaging technology to include lateral variations in lithology as well as tunnel and fracture detection, bedrock mapping, and subsidence/karst delineation has required a unique approach that incorporates SASW, MASW, and CDP methods. By integrating these techniques, 2-D continuous shear-wave velocity profiles of the subsurface can be generated. Estimating the dispersion curve from up to 60 closely spaced receiving channels located every 4 to 8 ft along the ground surface enhances the signal and results in a unique, relatively continuous view of shallow subsurface shear-wave velocity characteristics. This highly redundant method improves the accuracy of calculated shear-wave velocities (within 15% of measured, Xia et al., 2000) over other surface wave analysis techniques and minimizes the likelihood that irregularities resulting from erratic dispersion curves will corrupt inversion results.

Considering the sensitivity of the surface wave to changes in material characteristics, it is an effective first-order direct detection tool. By comparing changes in the propagation patterns of the wave-train anomalies associated with voids, changes in material composition, and even variation in bedrock depths can be ascertained. This method provides a quick, very non-unique method of identifying areas where the geology has changed, with depths that can be inferred from the $\frac{1}{2}$ -wavelength axiom and phase velocity estimation using the dispersive properties of surface waves from native, undisturbed, or “normal” earth materials.

Surface waves travel in a smooth retrograde elliptical fashion in a homogeneous earth. When anomalous material interrupts the otherwise laterally uniform earth materials the wavefield is disturbed, much like a rock disturbs the surface of a pond. Disturbances in the wavefield can be characterized based on radiation patterns of the surface wave after interacting with an anomaly such that the depth, approximate size, and lateral location can be estimated. Data for this kind of analysis are gathered in common offset, shot gather, or common receiver format with patterns associated with point source, linear, or volumetric changes in surface wave phase velocity characteristics enhanced with a variety of filtering techniques.

Model Studies for Voids

Abrupt, localized changes—either horizontally or vertically—in earth seismic velocities will alter the propagation pattern of seismic energy traveling through otherwise homogeneous earth materials. Perturbations in the propagation characteristics of seismic energy in the presence of such anomalous zones can be modeled to allow generalized differentiation of specific propagation characteristics, which are diagnostic of specific types of anomalies. Ground truth using real seismic measurements acquired over known target anomalies is also an important component in differentiating geologic noise from signal coming from a target anomaly. Using model-derived propagation characteristics in conjunction with calibrated ground truth seismic data, interpretation criteria can be established that allow high-confidence correlation between seismic observations on exploratory data and specific types of subsurface targets.

For the anomalies that were the target of this survey two different model scenarios and approaches were employed to better understand how the seismic energy would interact with targets in this geologic setting. First, a model was developed for the case of an anomaly with minimal horizontal extent (few centimeters) but with a large vertical dimension (10s of meters) (Figure 7). This model was designed to determine if the seismic wavefield was sensitive to the void volume or the boundary between the void space and native earth. A second model portrays a void that is 1 m high and 5 m wide (Figure 8). This second model configuration was designed to evaluate the impact the horizontal size of the void has in altering the seismic wavefield.

The first case might be geologically analogous to a fault zone or, of course, an extremely thin tunnel (Figure 7). Looking at surface wave energy only for this model, the presence of the anomaly is quite distinguishable on shot gather simulations over the anomaly when comparing to shot gather simulations with only uniform earth beneath the receiver spreads (Figure 9). As the simulated source and receiver spread advance across the model anomaly, changes in the arrival pattern of the surface wave

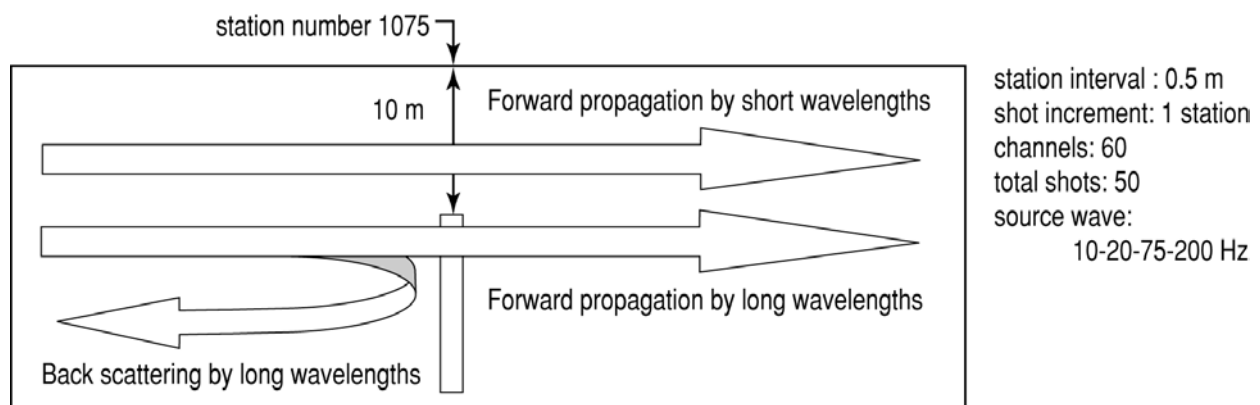


Figure 7. Model with arrows showing wave propagation and vertical void located at station 1075.

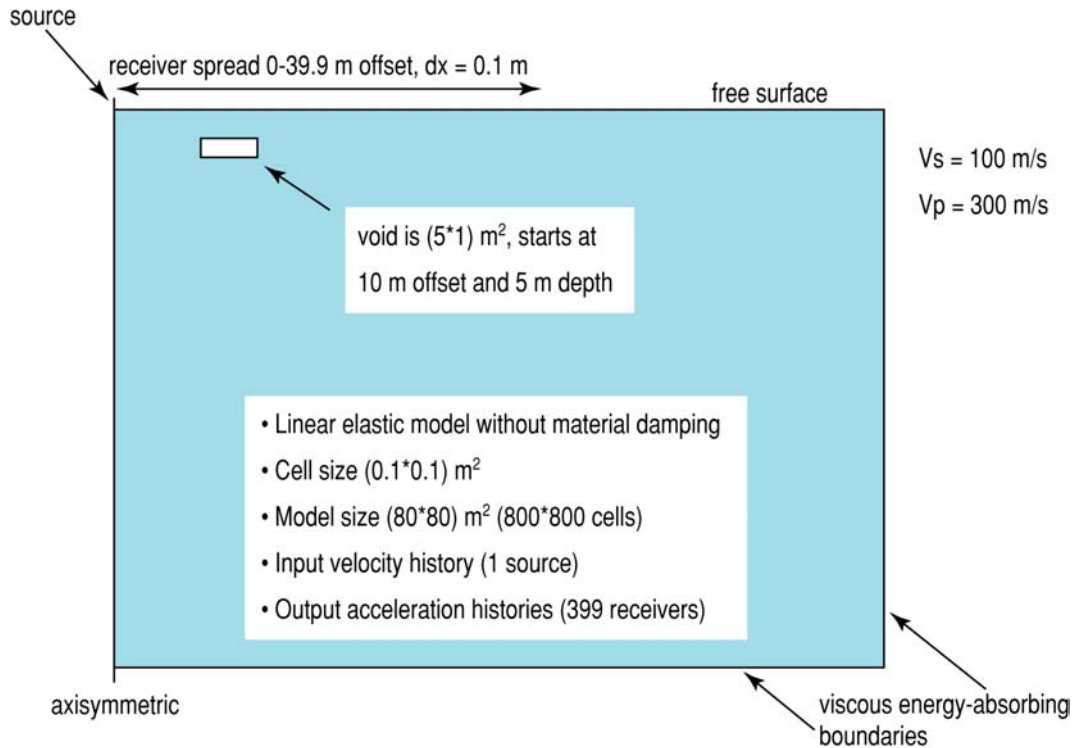


Figure 8. Void model using full elastic modeling routine. FLAC geometry.

energy are very evident. The width of the anomaly is obviously not as critical to the seismic response as the interface between native material and void space. Using the seismic wave pattern observed here it is possible to design a specialized processing flow that enhances energy that has scattered or reflected back after coming in contact with the interface between native materials and void space (Figure 10).

An important observation associated with this particular model of a thin, tall void is the effect that the depth to the top of the anomaly has on the seismic response. As the depth to the top of the void is increased from 1 m to 30 m the wave pattern remains constant, with only changes in frequency content and amplitude appearing to be depth dependent (Figure 11). Since this model represents native undisturbed material as homogeneous, the surface wave energy should not have any dispersive characteristics. The apparent dispersive characteristics of the backscattered or reflected surface wave seem to remain relatively consistent irrespective of depth to the top of the anomaly.

Studying the effect a vertically small void has on the seismic wavefield produces some intriguing observations (Figure 8). Surface wave energy passing through the model volume produces a seismogram with several very low amplitude events with apparent reverse phase velocities (Figure 12). Energy traveling back toward the source appears to originate from both walls of the model void. To enhance this apparent backscattered energy an f-k filter is applied to remove as much forward propagation surface wave as possible (Figure 13). Using this enhancement technique, two dominant reverse-traveling components of the surface wavefield become the highest amplitude events on the seismogram. Upon closer inspection it is evident that these events originate at the point in time when the surface wave passes through the contacts between the native material and void area. This suggests the surface wave energy is not particularly sensitive to the size of the void so much as the characteristics of the contacts between void and native material.

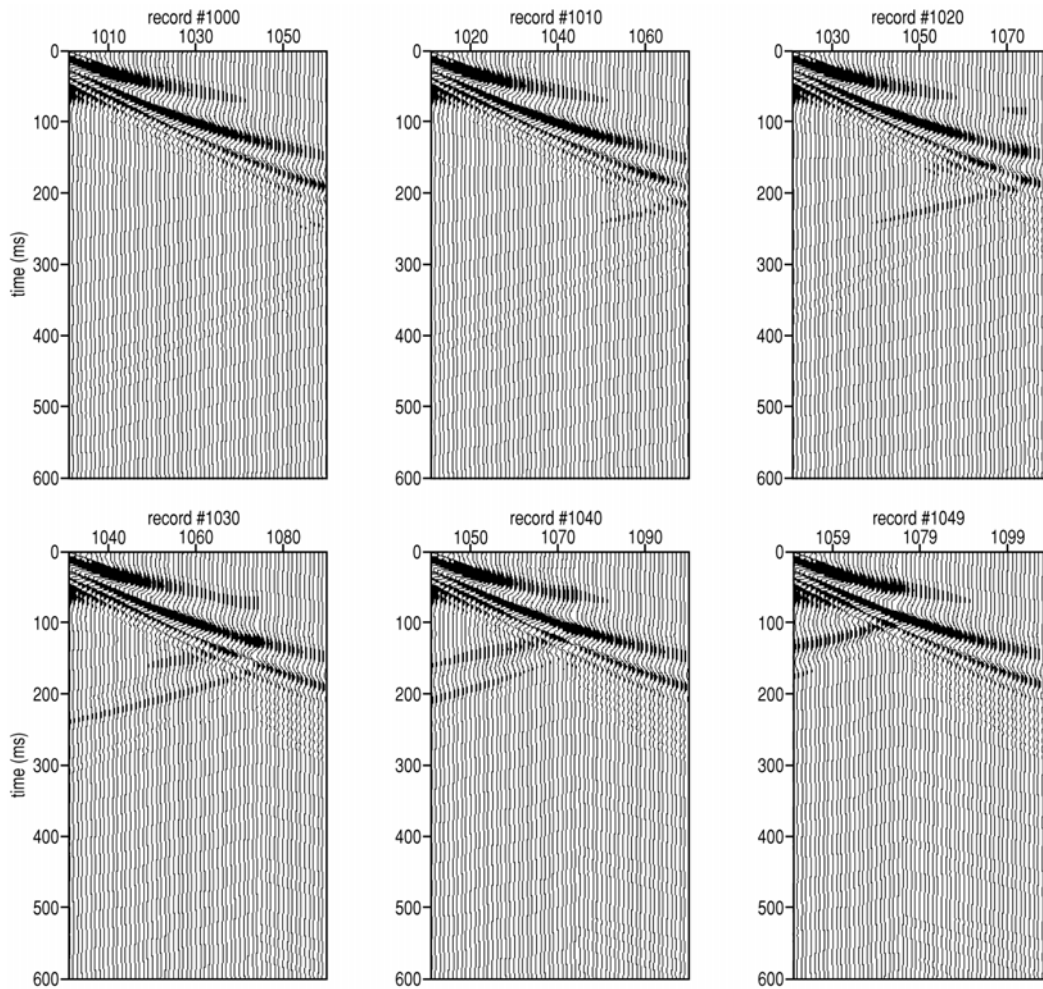


Figure 9. Selected model shot gathers as the source and receiver move across void.

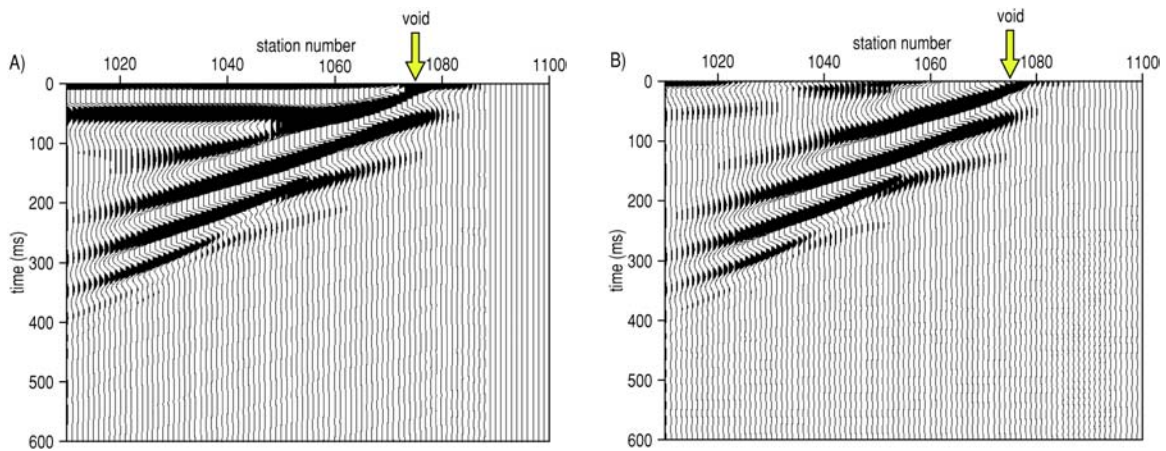


Figure 10. Void appearance after processing; void station = 1075. A) Processing to LMO sloping events consistent with dispersion curve; B) horizontal cut applied.

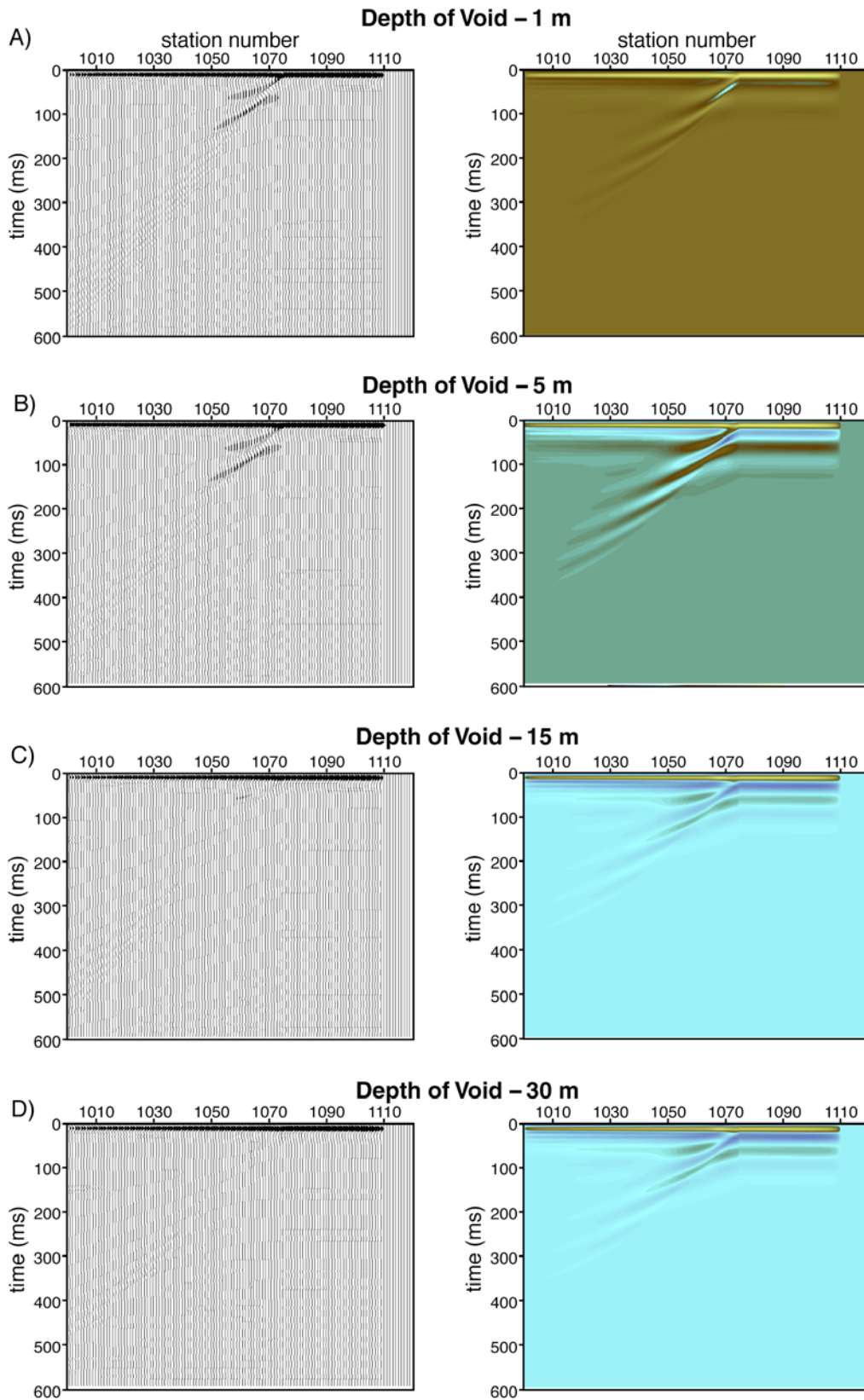


Figure 11. Model showing effect of void on seismic data as a function of increasing depth.

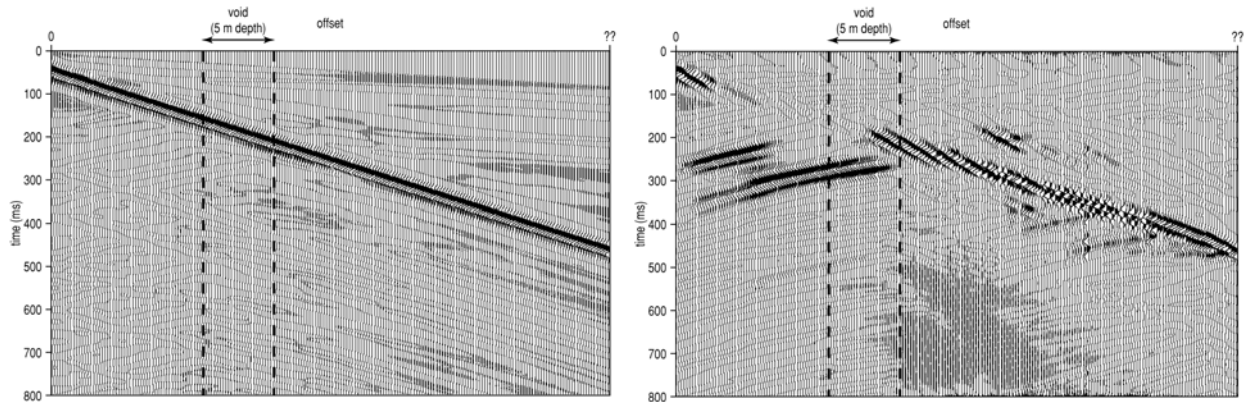


Figure 12. Shot gather from model shown in Fig. 8. Figure 13. Shot gather from model shown in Fig. 8. F-k filtering of forward propagation.

Field Procedures/Data Acquisition

Data were acquired for the 2-D full wavefield surveys at the three border sites visited during this campaign using state-of-the-art near-surface imaging equipment and techniques. Four Geometrics StrataView R60 seismographs were interfaced to a Geometrics StrataVisor NZC to allow the flexibility necessary to record from 1- to 240-channel configurations, each with 24-bit resolution (Figure 14). Because of the broad spectral requirements of full wavefield measurements it was necessary to use a low frequency source and matched low natural frequency receivers. Receivers were deployed in both a conventional spike-coupled format and a towed spread. In the spike-coupled format all receivers were Geospace GS-11D 4.5 Hz vertical geophones. For the towed array both Geospace GS-11D 4.5-Hz vertical geophones and Geospace GS-11 14-Hz horizontal geophones were towed in a continuous pressure coupled streamer (Figure 15). Receiver stations were spaced 1.2 m apart with the source impact points separated by 2.5 m for all seven survey lines. Three ground impacts from a rubberband accelerated weight drop (RAWD) were vertically stacked in the seismograph at each shot station (Figure 16).

Acquisition of the full wavefield data on this survey focused on generating and recording the broadest band data possible and tracking any anomaly that appeared continuous from the border north under U.S. territory. To reasonably image the full range of potential anomaly depths data needed to



Figure 14. Geometrics StrataView 240-channel seismograph with StrataVisor NZC mounted on a John Deere Gator.



Figure 15. 30-channel towed array along border fence.

include frequencies down to as low as 10 Hz with minimal interference from noise sources that propagate similar frequency seismic energy (large trucks, industrial facilities, heavy construction equipment, etc.). Night operations were determined necessary to maximize the signal-to-noise ratio in the presence of heavy commercial truck traffic moving along and across the border. Location and orientation of each line was designed first to optimally detect anomalies characteristic of tunnels crossing the U.S./Mexico border at near right angles to the border and, second, to best determine the orientation and northern extent of each specific anomaly interpreted to penetrate the border using line-to-line correlations. Full wavefield data acquired for surface-wave analysis (inversion, linear moveout and common receiver stack, and backscatter enhancement processing) was also used for tomography and refraction studies.



Figure 16. RAWD impulsive seismic source dragging towed spread.

Data were acquired at three sites along the border (Figure 1). Two sites were selected as candidates for potential tunnel crossings based on intelligence, and in the case of the Otay Mesa, California, Port of Entry site, a vertical shaft discovered on the Mexican side of the border in January 2003 narrowed the search aperture. The third site is the location of a known tunnel discovered in the mid-1990s which was successfully detected at its northern extreme using seismic techniques in January 2002. Since the tunnel is only 35 ft deep where it was seismically detected back in January of 2002 (Miller et al., 2002), it was necessary to calibrate the seismic tool further south where the tunnel was known to be over 65 ft below ground surface and where the background noise was similar to that expected at the two search sites suspected to be above tunnel crossings. Test results from the known tunnel site were critical to generating a tunnel seismic signature template that, in conjunction with model results, were used to differentiate anomalies that were tunnel candidates from those that were related to geologic or cultural features.

Processing Focusing on Void Seismic Characteristics

Processing concentrated on data recorded from 30 vertical receiver stations optimally offset from the source by a range of distances determined during preliminary testing at the known tunnel site with confirmation of the selected range of offsets at each site. All processing was centered around wavefield anomalies caused by small voids in otherwise relatively uniform earth materials less than 100 ft below the ground surface. Traditional approaches to surface wave processing were used to estimate dispersion characteristics and to designate the acquisition geometries and operational procedures. In-field processing was critical to the overall quality of the data (signal-to-noise, spectral characteristics, and optimum range of recorded offsets) (Figure 17).

Analysis of dispersion curves (frequency vs. phase velocity) and shot gathers (scattered energy, non-linearity of wave propagation, and frequency vs. source offset) provided a variety of different approaches to enhancing the empirical and model-derived seismic characteristics of voids. Data were analyzed and processed using beta versions of both



Figure 17. On-site processing facility mounted on semi truck.

SurfSeis and WinSeis Turbo (proprietary software packages from the Kansas Geological Survey facilitating use of MASW as well as general seismic data processing). The dispersive characteristics of surface waves and their retrograde elliptical particle motion that has 3-D characteristics provides for a variety of processing in interpretation techniques based on the sensitivity of all seismic energy to abrupt changes in seismic velocity and/or density, such as a layer or wall. These data were run through a large and diverse set of processing routines with the most notable listed below:

- offset-dependent estimations of dispersion curves,
- inversion of dispersion curves to establish velocity depth dependencies,
- linear moveout as a function of phase velocity in the f-k domain,
- filtering in the f-k domain all energy not consistent with normal surface wave propagation in a homogeneous earth in both shot and receiver domain,
- common receiver stacking after linear move-out (LMO) and receiver gathers for different offsets,
- digital filtering pre- and post-LMO and receiver stack,
- Vs cross-sections from inversion of dispersion curves,
- filtered dispersive seismic events (FDSE) pre-receiver stack, and
- grid-dependent migration of all potential back scatter points.

To increase the signal-to-noise ratio and to improve convergence during inversion, a new technique called Filtering of Dispersive Seismic Event (FDSE) was used to suppress higher modes on some shot records (Park et al., 2002). This method removes higher modes through filtering in the frequency domain and avoids the detrimental artifacts that are observed in dispersion analysis if higher modes are removed using time-domain muting (Ivanov et al., 2001).

Many more processing and signal enhancement techniques were experimented with on data acquired at the suspected tunnel sites. The previously listed processing routines resulted in the greatest enhancement of first-order tunnel seismic energy arrivals as predicted by modeling and empirically observed on the calibration data over the known tunnel site.

Interpreting Voids

As is the case with all geophysical methods, no single data set can provide a unique answer or solution. All seismic data is non-unique. Therefore, to best provide a defensible, confident interpretation it is important to first construct numerical models and synthetic seismic data based on best estimates of target characteristics and second, if possible, acquire data at a site with similar geology and a known feature closely resembling in depth and size the survey's target feature. By establishing a "seismic template" in this fashion, pattern recognition and associated assignment of candidate features with confidence ratings can be effectively done.

Data were first acquired on this tunnel search mission above the 1200 ft long tunnel discovered in the mid-1990s passing 65 ft beneath the border fence and shallowing to 35 ft near the planned exit point. The tunnel was discovered before it could be completed, but serves as an excellent physical model that likely resembles other tunnels that might be present or planned in this area (Figure 18). Processing that most strikingly



Figure 18. Otay Mesa tunnel at ~45 ft below ground surface.

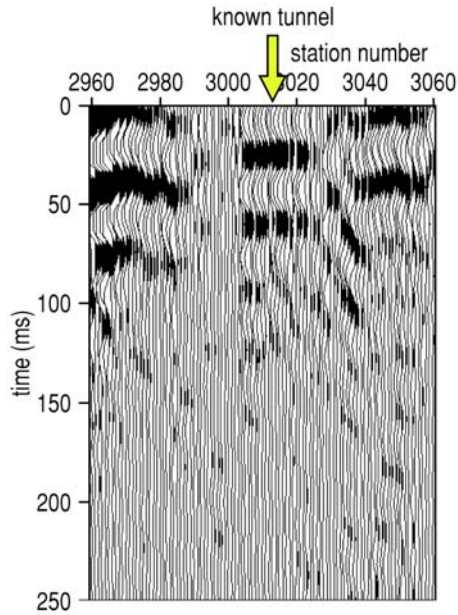


Figure 19. Line 3, test line with known tunnel. Bandpass (5-10-20-35 Hz) + horizontal cut.

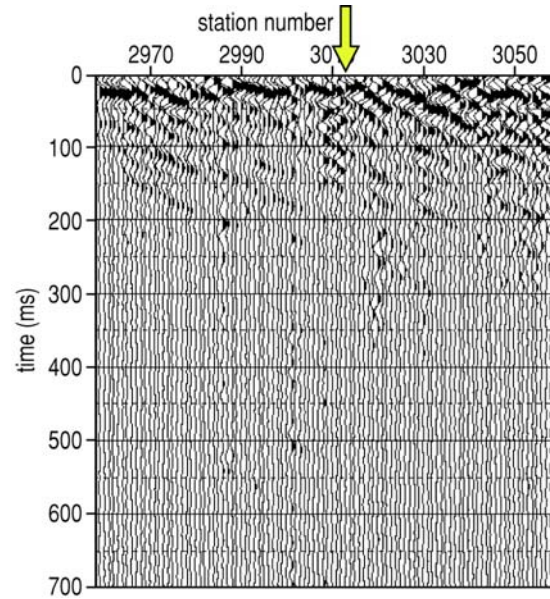


Figure 20. Line 3, 47 ft north from the tunnel shaft. Tunnel is located at station 3013.

enhanced signal interpreted to have returned from the known tunnel included LMO (as a function of phase velocity and frequency), common receiver stack, and spectral bandpass filtering (Figure 19). Enhancing the east-sloping energy arrivals further was possible using a pre-stack f-k filter to remove all horizontal energy (Figure 20). With the progression of the source from left to right or west to east across the tunnel, the only energy arriving after this processing flow with a slope from west to east will be backscatter or reflected energy. Using the model-predicted slope and pattern of tunnel-specific energy as a guide, it appears the known tunnel site produces a distinctive and interpretable tunnel signature above the tunnel when it is 65 ft below ground surface that is consistent with the one observed when the tunnel was 35 ft below ground.

With confidence based in how well the numerical model correlates to the physical model (known tunnel site), the search for seismic anomalies moved to the suspected tunnel site located immediately south of the Otay Mesa, U.S. Customs, Port of Entry (POE) (Figure 1). Four lines were acquired at this site, two south of the POE (Figure 21) and two north (Figure 22). The two southern lines were acquired in distinctly different surface settings. The lines north of the POE were joined, with line 10 being a westward extension of line 6.

Line 4 was acquired from west to east (Figure 23) and then repeated from east to west (Figure 24). This duplication in subsurface sampling was designed to verify that anomalies interpreted as potential targets were not related to source-to-receiver orientation but to subsurface anomalies with characteristics consistent with voids. The dominant anomaly that most closely matches the void seismic template can be identified beneath station 4052 on both data sets. Data from line 4 were processed to enhance backscattered or reflected arrivals, and therefore any energy arrivals with dominant slopes opposite the source radiation pattern (west to east for Figure 23 and east to west for Figure 24) represent a potential anomaly. A second anomaly identified beneath station 4005 on the west-to-east profile possesses similar sloping arrival patterns as those observed beneath station 4052 (Figure 23). The anomaly beneath station 4005 has a significantly greater vertical expression in time than predicted by models or seen on the physical model data. This anomaly has been tentatively interpreted as near-surface related.

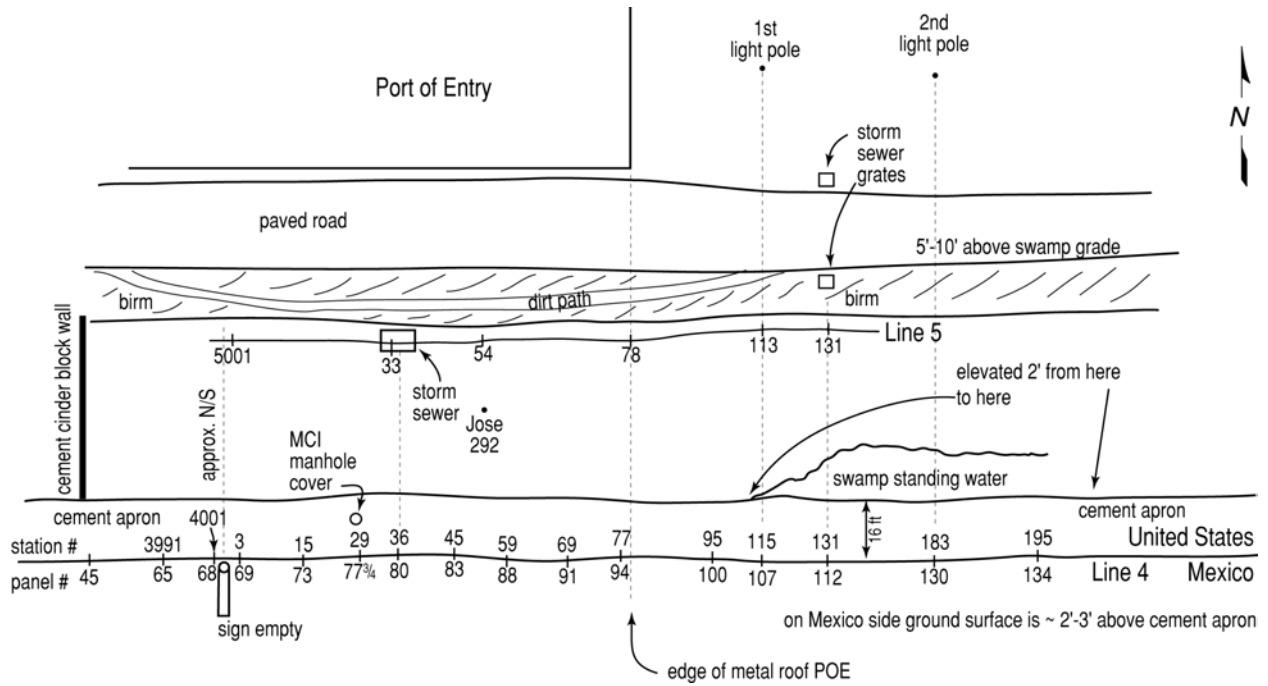


Figure 21. Detailed site map with stations tied to panel numbers and facilities.

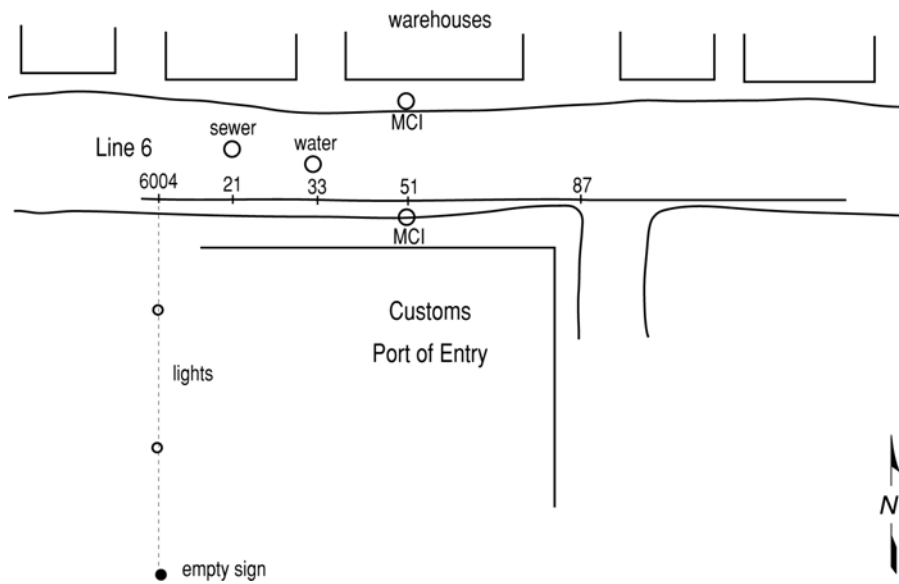


Figure 22. Site map with station numbers tied to permanent features.

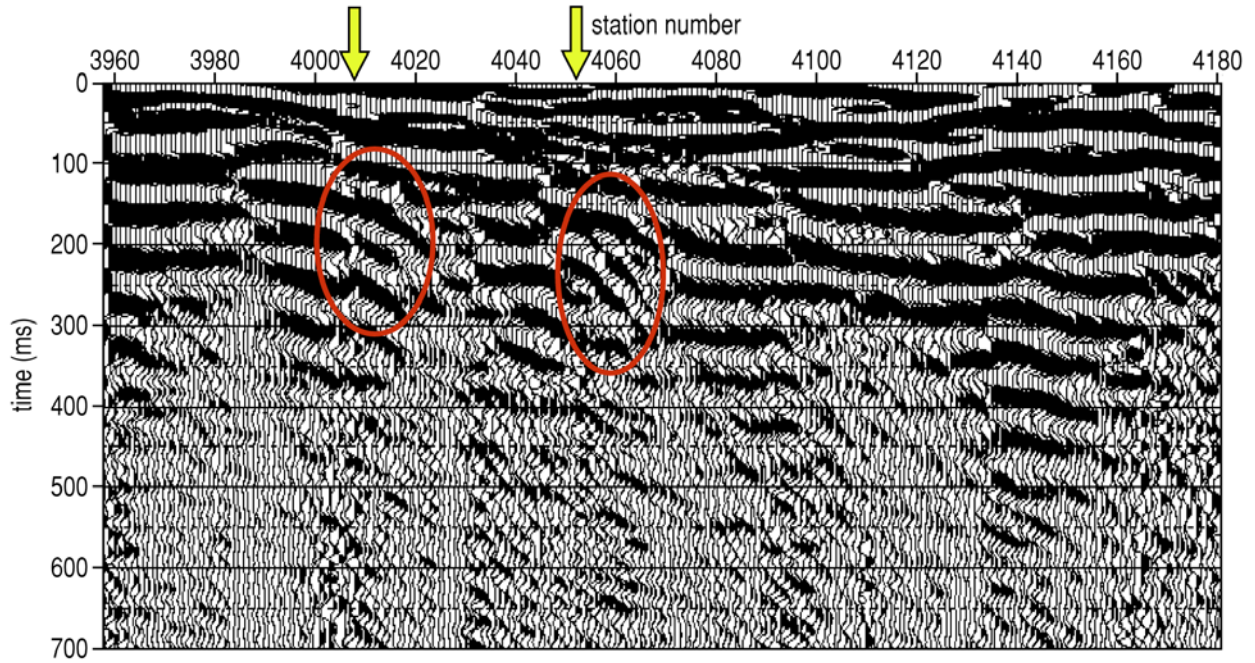


Figure 23. Line 4 processed to enhance scatter.

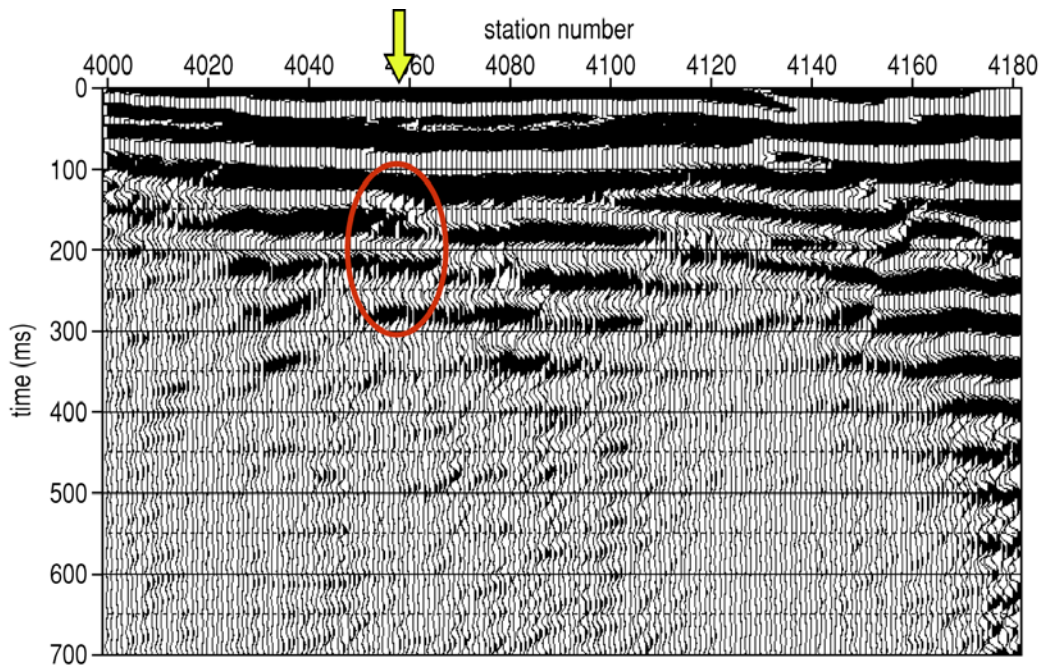


Figure 24. Line 4R (reverse), at the border fence on the concrete way. Unknown tunnel location.

More advanced processing of line 4 data produces an even more convincing image that can be interpreted as suggestive of abrupt velocity contrasts in the subsurface. Back scatter events beneath about stations 4080 and 4090 are clearer and appear easier to interpret on the east-to-west profile when an f-k filter is applied before common receiver stack (Figure 25). When f-k filtering is applied to shot gathers acquired from west to east the two anomalies interpreted at 4052 and 4078 become quite pronounced with some indication an anomaly at 4090 was interfering with the one at 4078 (Figure 26). From the same data set (Figure 26) when only offsets between 80 and 128 ft from the source are included, subtle arrivals indicative of a void or a localized velocity contrast are interpretable beneath about station 4010 or so (Figure 27) an anomaly also interpreted on Figure 23. Considering all the data and processing flows, it seems reasonable to suggest four anomalies with characteristics that in some way, shape, or form are consistent with the tunnel template. These include stations 4052, 4078, 4005, and 4090, each of course meeting the criteria for target anomalies to differing degrees.

Line 5 provided no data that are useful in searching for tunnels in this area. These data were acquired using spike-coupled geophones in the marshy area between the border fence and truck access road between the POE and California Department of Transportation Weight and Inspection station (Figure 22). Soft, marshy ground is notorious for not being conducive to the generation or propagation of low-frequency surface waves. However, the processed sections from line 5 provide an excellent seismic image of the culvert that passed between the source and receivers located at station 5033 (Figure 22). The scatter pattern and apparent “pull down” in the otherwise linear event at about 75 ms observed on the processed sections are very diagnostic and unique compared to most other anomalies interpreted on data during this survey (Figure 28). The lack of broadband surface wave energy and the separation between source and receiver locations inhibited the ability of line 5 data to possess the subtle anomalies that have been identified as potential target anomalies on line 4.

Any tunnel crossing beneath the border near the POE, intended for use by traffickers in illegal people and/or goods, would require an exit point on the U.S. side of the border that is hidden from view. The nearest potential exit points along this stretch of the border are the warehouse type structures immediately north of La Amistad street and adjacent to the POE (Figures 22 and 29). Line 6 and 10 were acquired to intersect the most likely paths of tunnels crossing lines 4 and 5 in route to those structures. Data from line 6 and 10 were optimally acquired to search for anomalies consistent with the void/tunnel seismic template and that could be correlated to similar anomalies on lines 4 and 5 located within 100 ft of the border fence (Figure 21).

Another important consideration from a tunnel construction perspective is the need for alignment. Keeping the tunnel straight minimizes the length necessary to reach the intended exit point and insures emergence at the designated location. Some form of surveying is necessary during construction. The simplest and the method used during construction of the known tunnel at Otay Mesa, California, relies on line-of-sight. From the known vertical shaft a warehouse on the Mexican side of the border (M1, Figure 30) obstructs line of sight for all seismic stations larger than about 4130 while the POE main building obstructs the line of sight for all stations smaller than 4010. Between stations 4010 and about 4050 line of sight is possible but structures on the POE facility inhibit a clear view of the row of warehouses north of the POE.

Initial analysis of the processed data from lines 6 and 10 reveals two unique anomalies that can be interpreted on all the various enhanced, processed versions of line 6 with two anomalies interpretable when the shot gather data is f-k filtered after LMO and before common receivers stacking (Figures 31-34). These anomalies are consistent with the model-derived seismic template with respect to apparent arrival slope, general frequency relationship, attenuation characteristics, and verticality of cyclic arrivals.

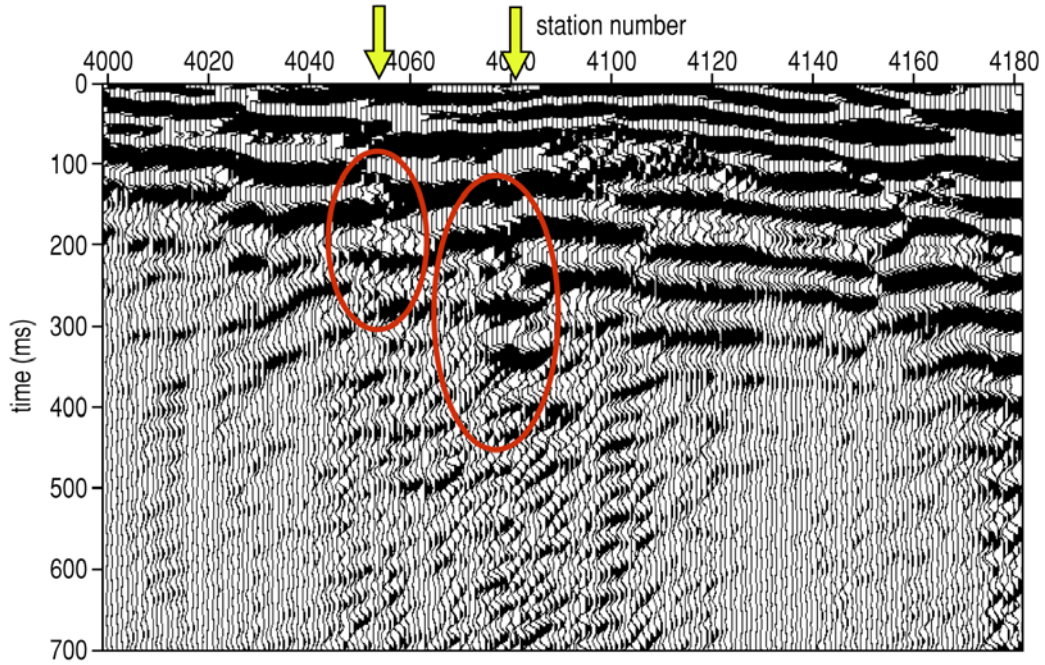


Figure 25. Line 4R (reverse), at the border fence on the concrete way, with horizontal f-k filter applied. Unknown tunnel location.

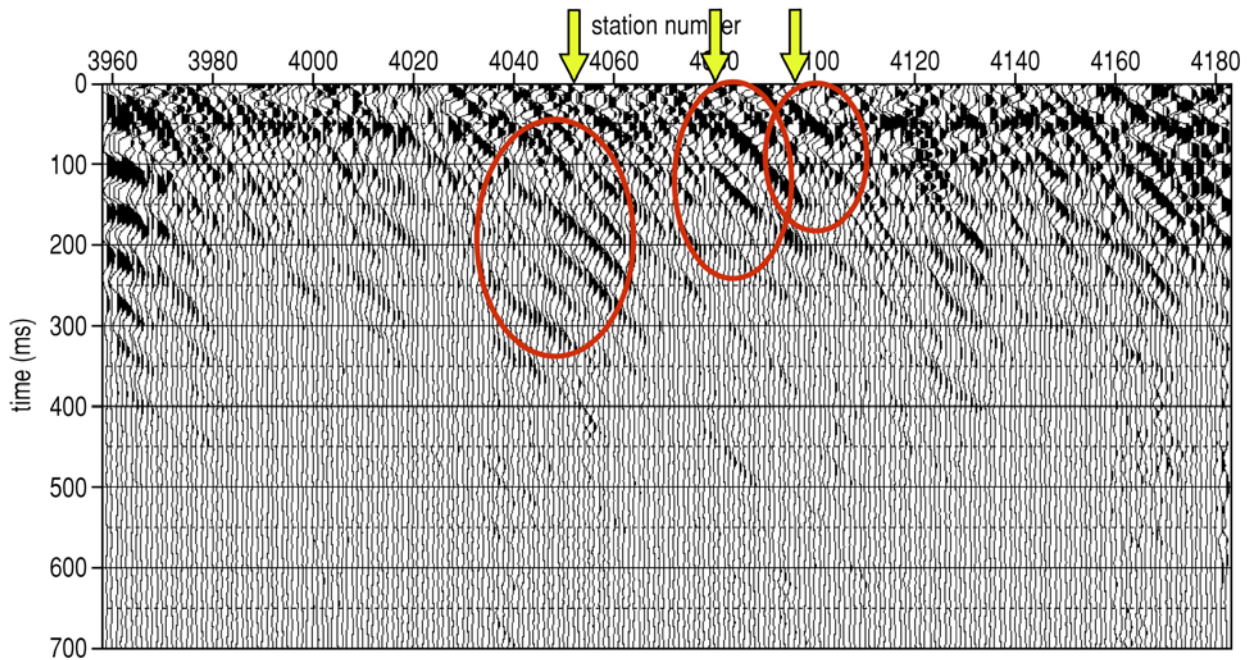


Figure 26. Line 4, at the border fence on concrete way, after f-k filtering of shot gathers. Unknown tunnel location. Possible backscatter from tunnel indicated with red circle centered on about station 4048.

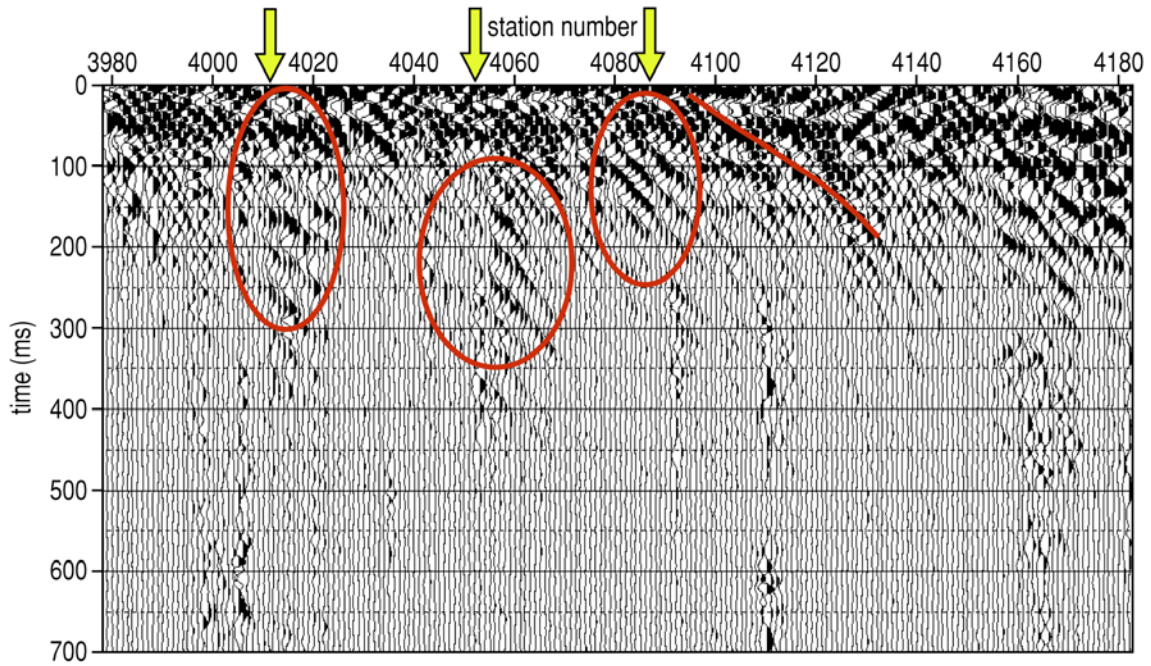


Figure 27. Line 4, at the border fence on concrete way, after f-k filtering of shot gathers, offsets 80-128 ft. Unknown tunnel location. Possible backscatter from tunnel indicated with red circle centered on about station 4055.

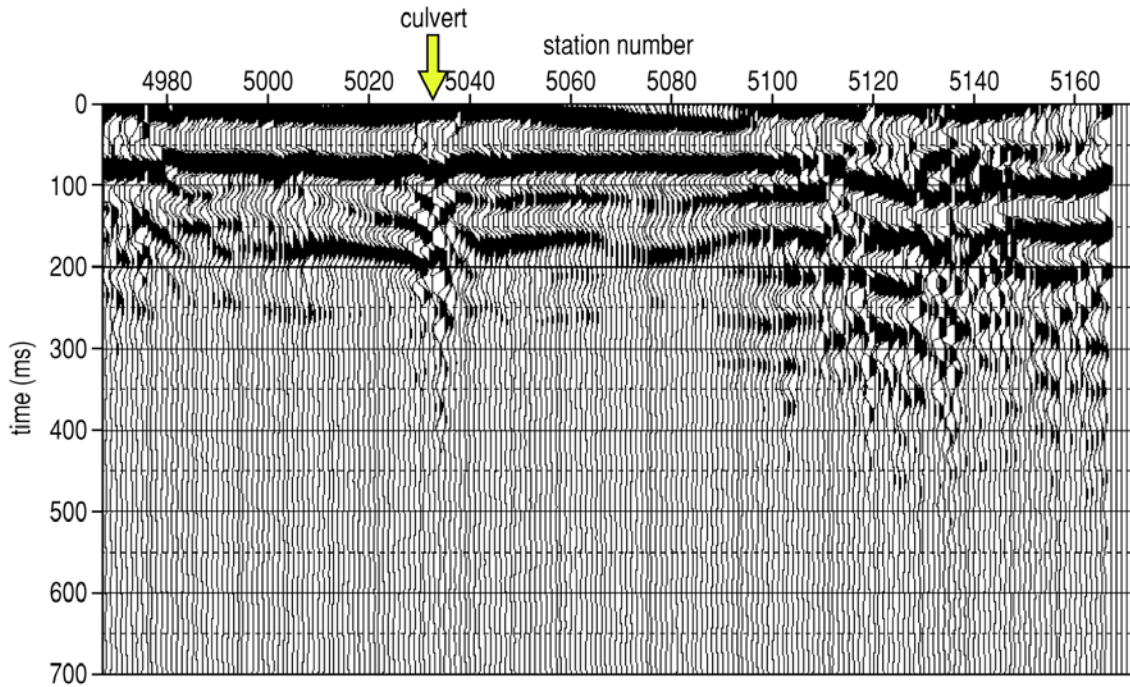
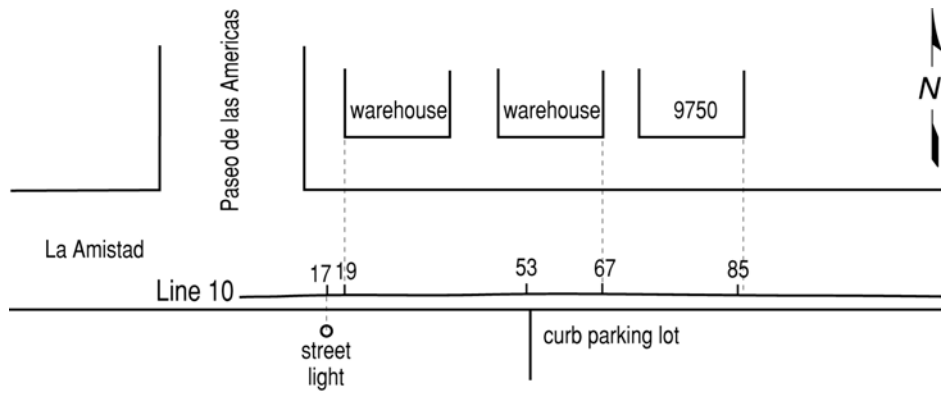
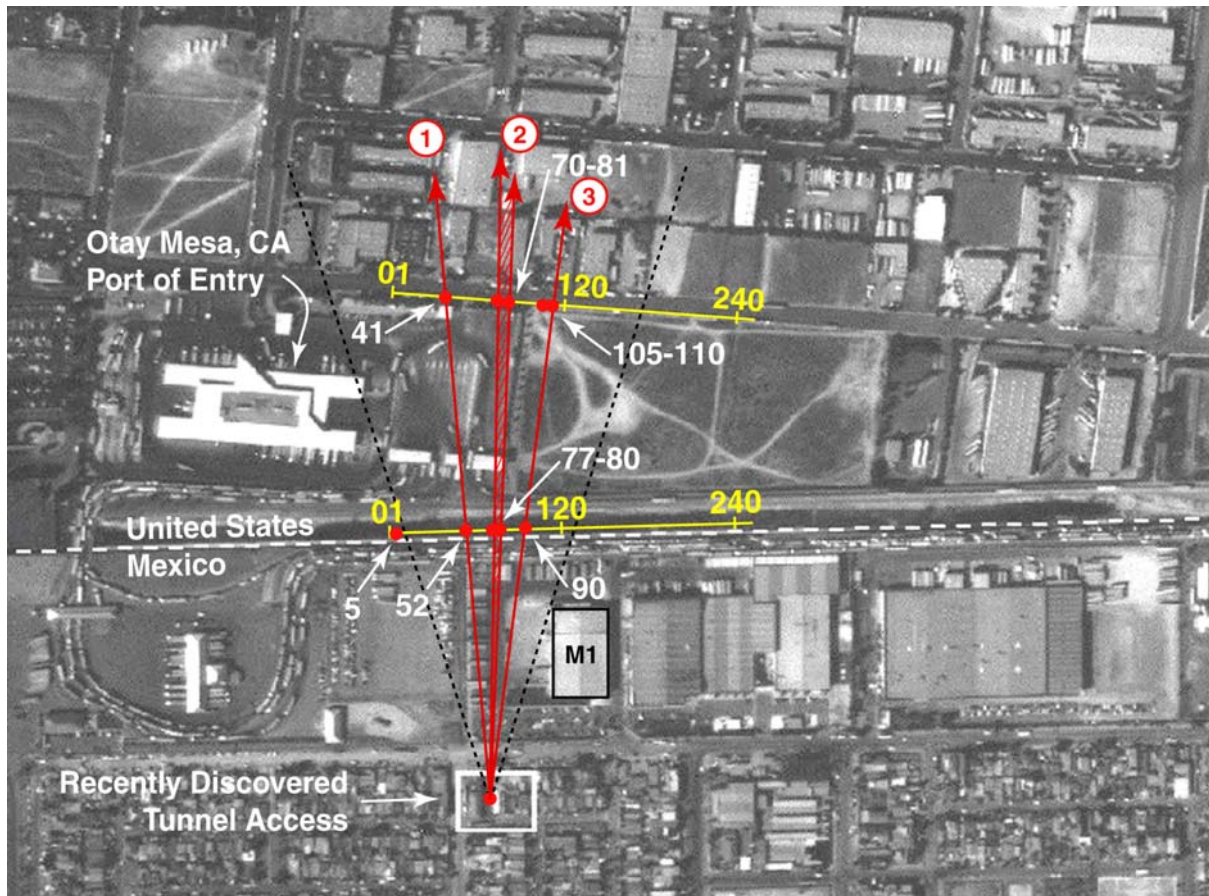


Figure 28. Line 5, at the border fence, geophones in swamp, source between swamp and road. Unknown tunnel location. Culvert under road at approximately station 5033.



Port of Entry, Otay Mesa

Figure 29. Detailed site map with station locations tied to semi-permanent surface features.



---- line of sight boundary — possible track of tunnel ① probability ranking: 1 = most likely, 3 = least likely

Figure 30. Aerial photo with seismic lines and possible extrapolations of continuous subsurface anomalies, Otay Mesa, California.

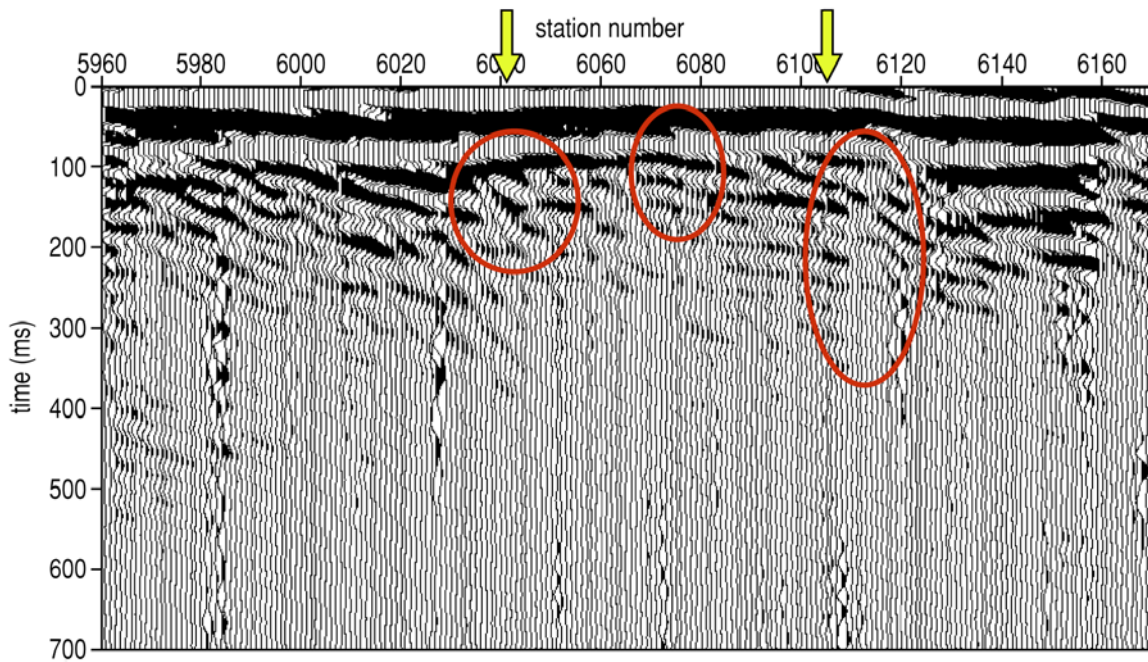


Figure 31. Line 6 on asphalt street.

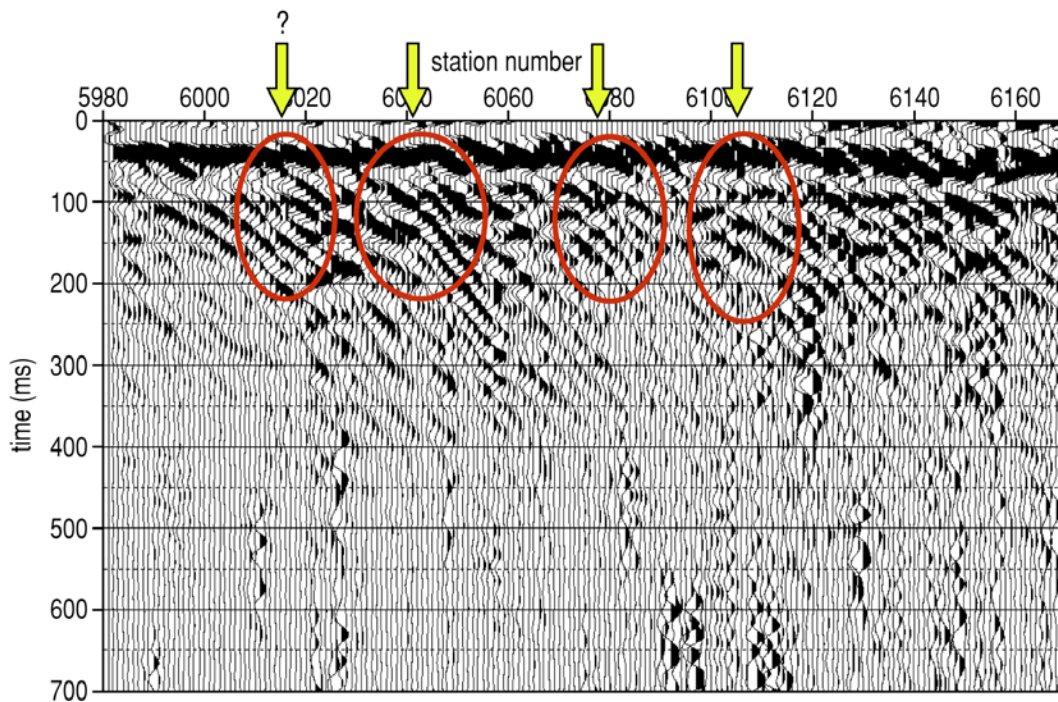


Figure 32. Line 6, on asphalt street, f-k filtered shot gathers. Location of the tunnel-suspect wave patterns observed on the shot gathers.

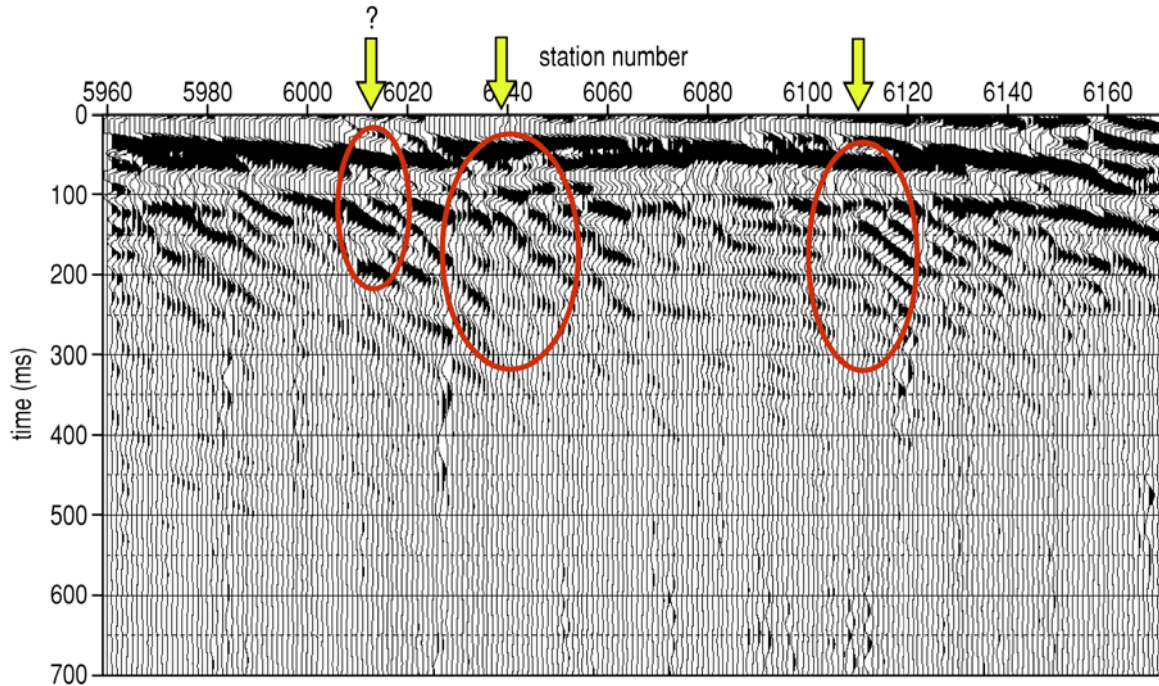


Figure 33. Line 6, on asphalt street, f-k filtered shot gathers. Location of the tunnel-suspect wave patterns observed on the shot gathers.

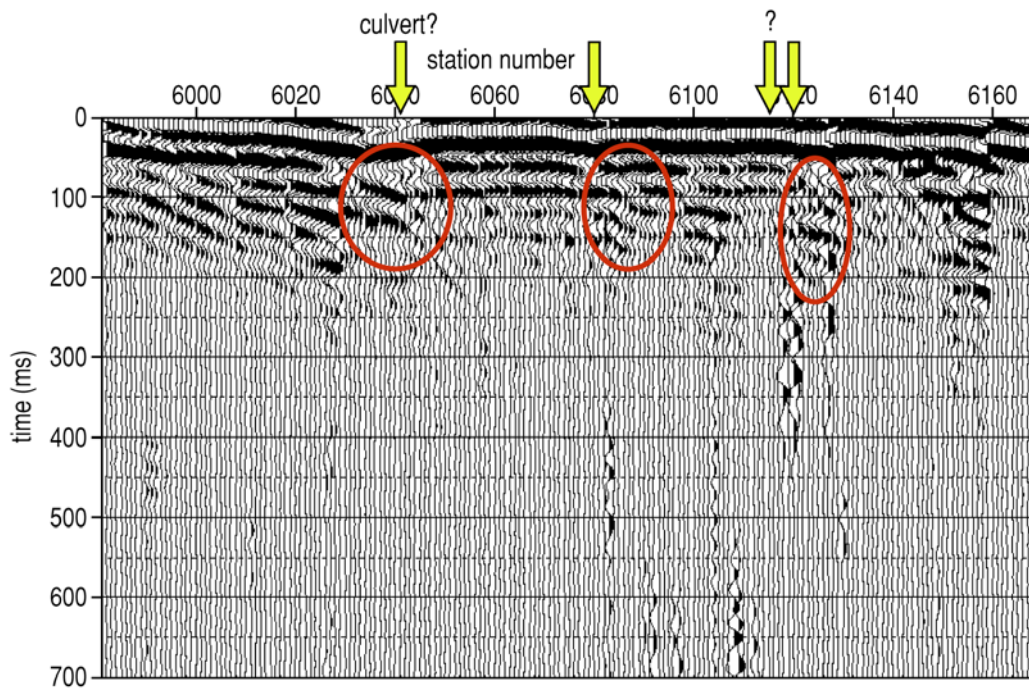


Figure 34. Line 6, on asphalt street. Offset range 52-48 ft. Location of the tunnel-suspect wave patterns observed on the shot gathers.

A confidence estimate made for each of the four anomalies on line 6 is based on how well in a qualitative sense they match with the models and with a reasonable linear trace between the known vertical shaft and anomalies on line 4. Probably the best match is 6041, which aligns quite well with 4052. A larger and less concise anomaly is interpreted between stations 6070 and 6081. The large range of this anomaly is a direct result of its more chaotic arrival pattern, which, based on modeling, could be indicative of a wider feature. The last two anomalies on line 6 are fair to at best good and are located between stations 6105-6110 and at station 6010; neither has a clear mate on line 4.

Using straight-line tunneling techniques, line of sight survey methods, and potential evasion of passive seismic monitoring, the most likely path a tunnel takes (if it exists at all) is along a line from the tunnel access vertical shaft, through station 4052, under the POE, across La Amistad beneath station 6041, and emerges in one of the row of warehouses immediately north of La Amistad (Figure 30). The second most likely path again starts at the vertical shaft and moves north under the border and line 4 between stations 4077 and 4080, then north under the extreme east end of the POE facility, across La Amistad between stations 6070 and 6081, and into one of the warehouse in the block immediately north of La Amistad. A third set of anomalies that might be indicative of the trace of a tunnel are 4090 and 6105 to 6110. Line 4 data for this third set does not possess nearly as strong an arrival pattern, but it is very consistent with the shape of the arrival pattern from the known tunnel site on line 3. The other anomalies interpreted on lines at this site are also tunnel candidates; however, they don't possess all the characteristics that would allow line-to-line correlations nor do they have convincing arrival characteristics to make them a priority anomaly.

Shot gathers were used as a diagnostic tool for directly detecting abrupt changes in an otherwise uniform earth (Figure 35). As can be seen on shot gathers from line 5 (Figure 35 (A)) the culvert located beneath station 5033 possesses a pronounced scatter consistent with the model data and with a scatter feature on line 6 beneath about station 6040 (Figure 35 (B)). The unique curvature of these scatter features is not particularly diagnostic of tunnels, but it is diagnostic of abrupt changes in velocity. Shot gathers were used in conjunction with processed records to establish confidence in observed scatter events on stacked sections.

A second site was investigated as a potential tunnel crossing area near the town of San Ysidro, California (Figure 1). Based on intelligence, the Corona Beer Warehouse was the proposed entry point on the Mexican side of the border. With the warehouse only a hundred feet or so from the fence, data acquisition focused on a 600 ft stretch of the border centered on the warehouse and extending from the border fence to just north of the Ballard fence (Figure 36). The presence of a major highway to the coast from Tijuana, Mexico, resulted in high levels of background noise and required night operations for line 8. Due to safety concerns, day operations were re-implemented for line 9.

Line 8 was acquired at night parallel to and north of the Ballard fence and approximately 150 ft from the border fence (Figure 36). Raw shot records possessed indications of a scatter event from around station 8066. Processed, full wavefield data, including LMO and common receiver stacking, have subtle indications of backscattered energy along a sizeable portion of the profile (Figure 37). The highest amplitude scattered energy is concentrated beneath station 8064 with another, much lower energy burst around station 8158. With enhancement processing that includes f-k filtering of all flat arrivals, the two seismic events previously evident become obvious (Figure 38). When close offset traces are removed prior to common receiver stack, the obvious events become standouts (Figure 39). From these records it is reasonable to suggest that 8064 has the greatest likelihood of being a tunnel type anomaly with 8158 being possible, but much less likely.

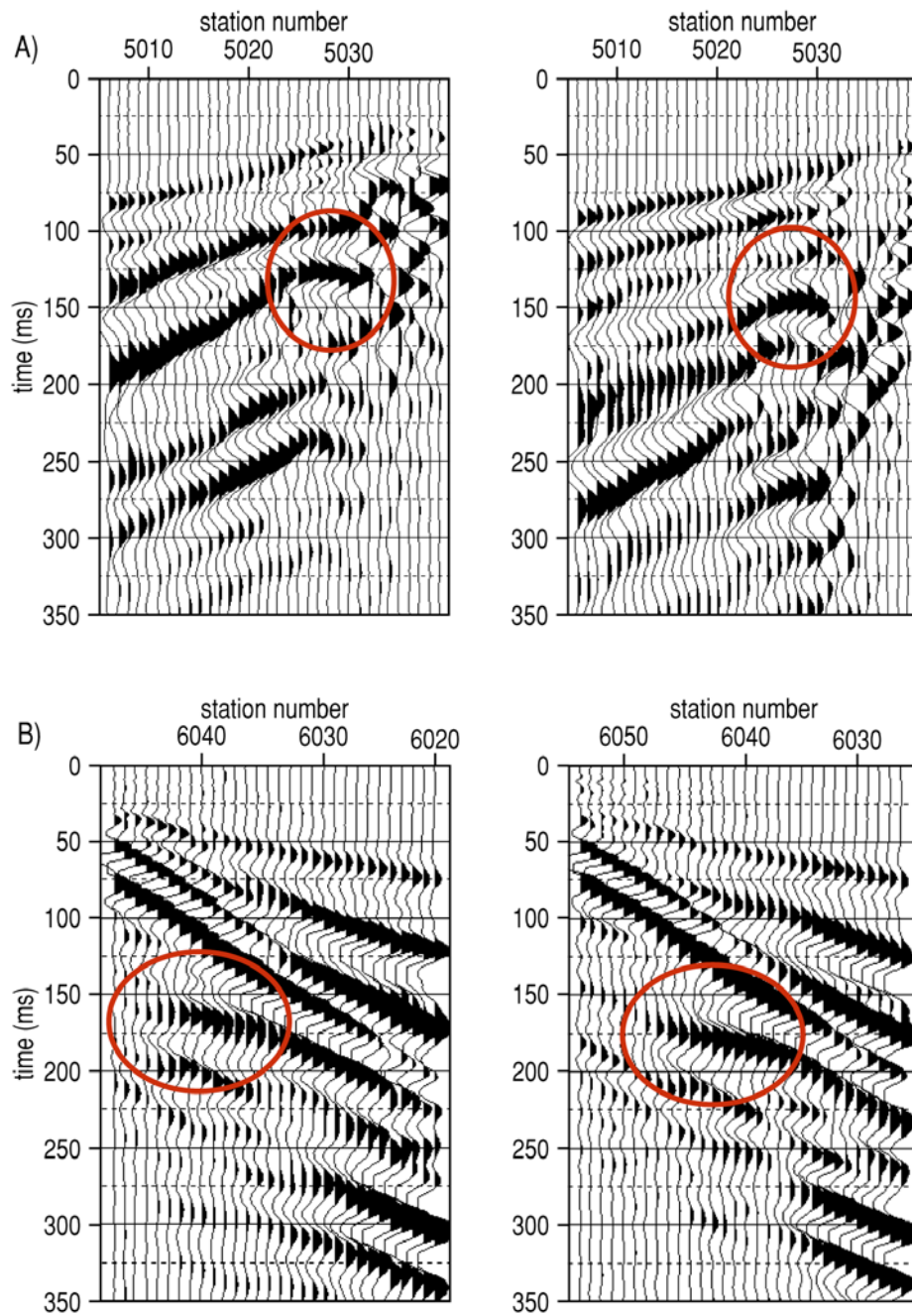


Figure 35. Shot gathers from (A) line 5 and (B) line 6 showing tunnel-suspect wave patterns.

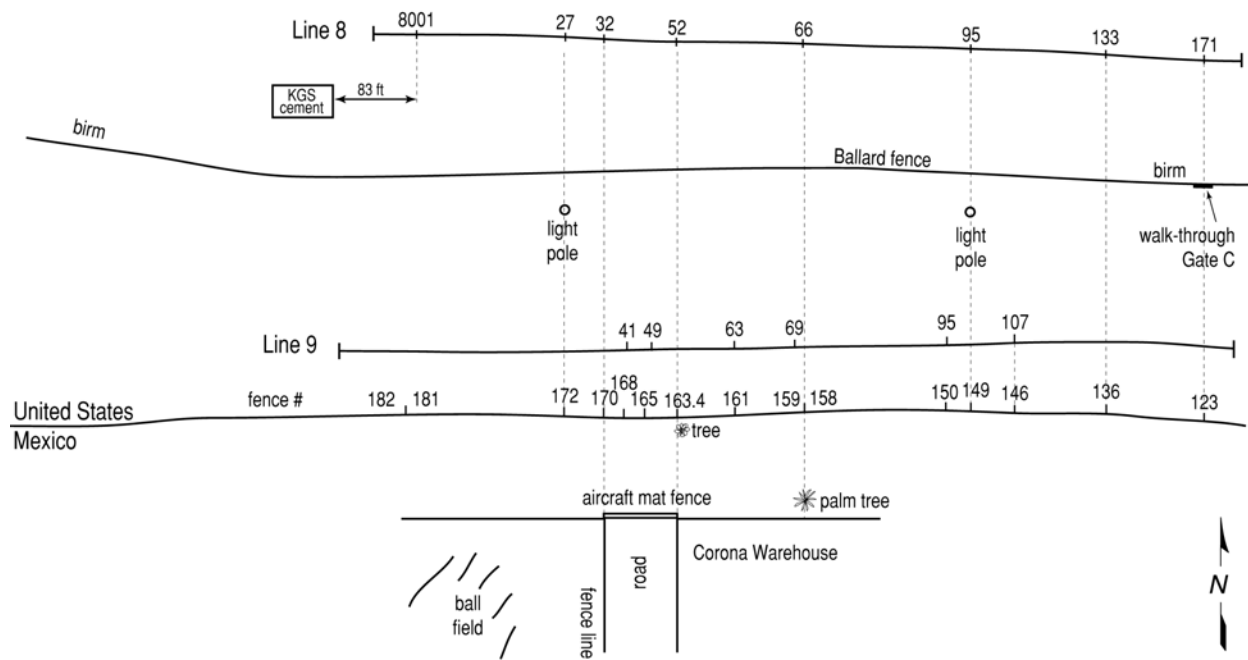


Figure 36. Detailed site map from San Ysidro, California, site. Stations are tied to panel numbers and features on Mexico side of border.

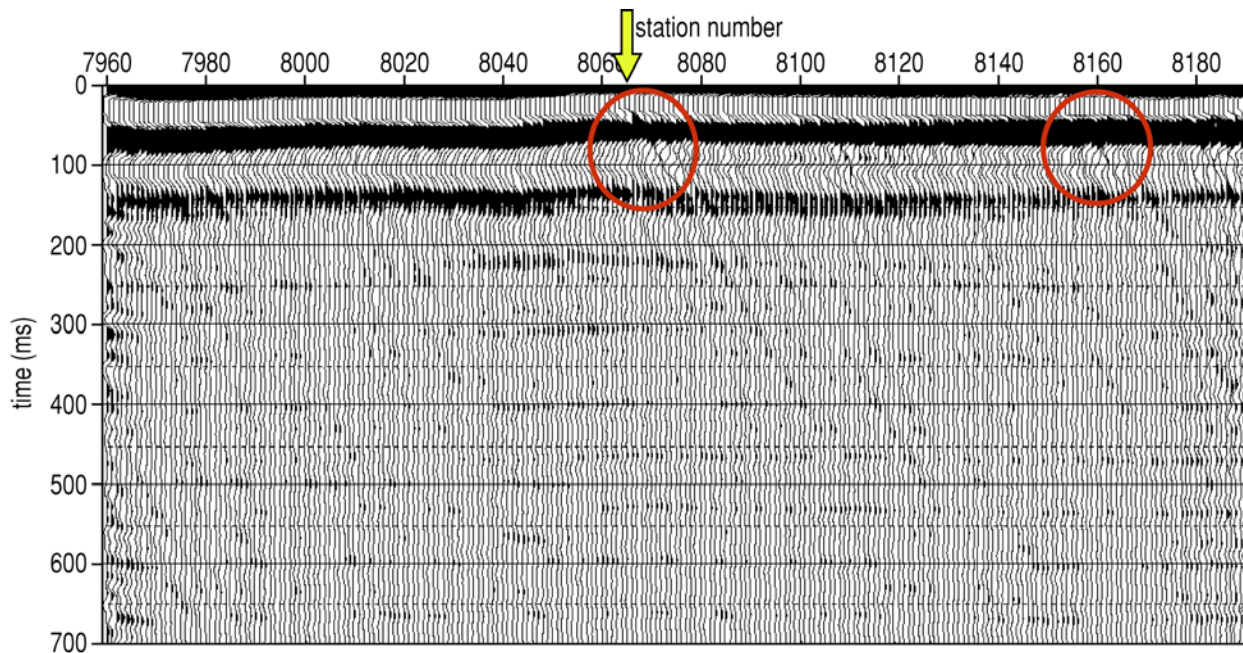


Figure 37. Line 8, north of Ballard fence, near Corona Beer Warehouse.

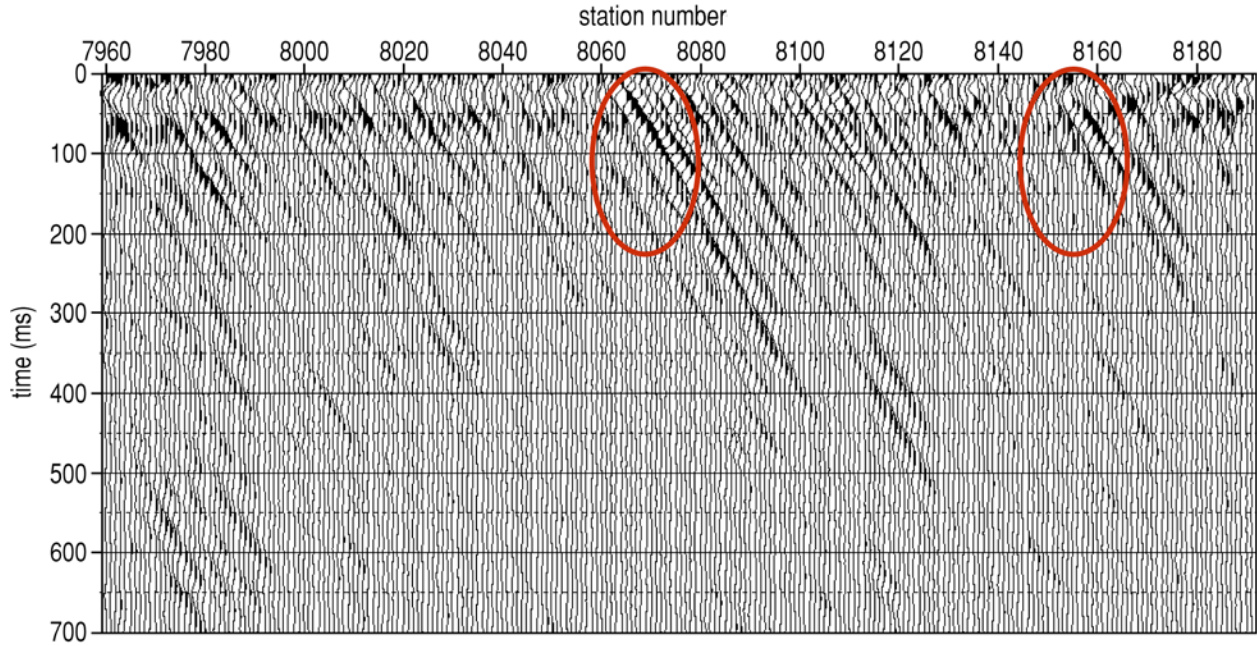


Figure 38. Line 8, north of Ballard fence, near Corona Beer Warehouse. After f-k filtering.

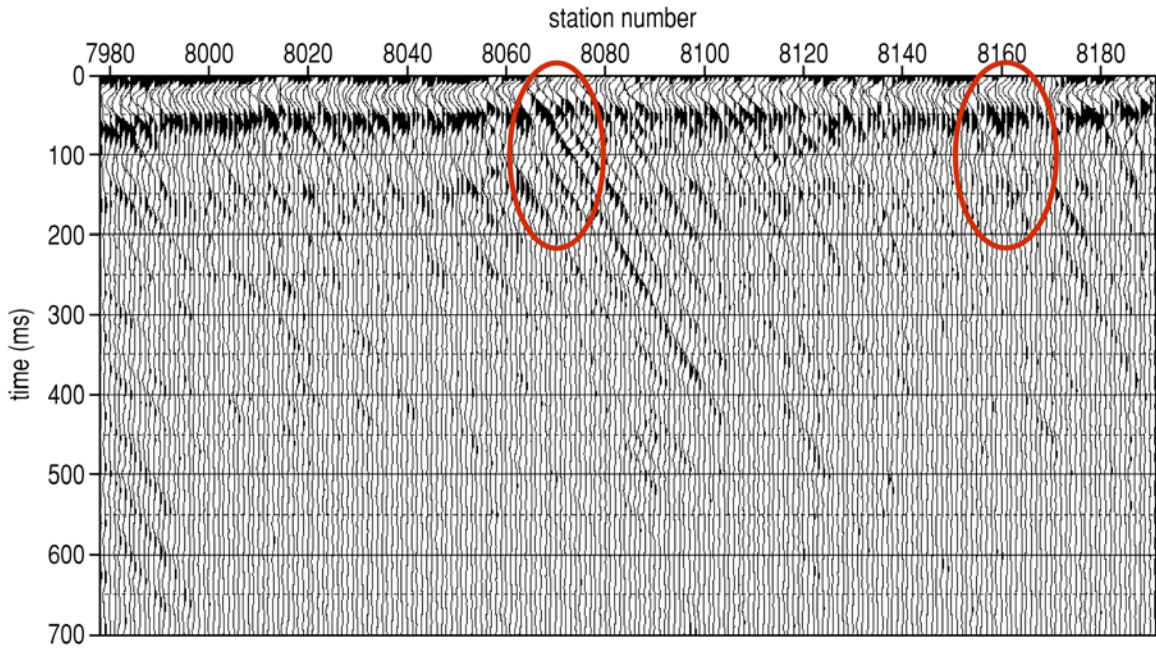


Figure 39. Line 8, north of Ballard fence, near Corona Beer Warehouse. After f-k filtering, offset range 92-128 ft.

With line 8 and line 9 in proximity and with the anomaly identified on line 8 at station 8064—reasonably consistent with the center of the warehouse—an anomaly on line 9 around 9065 would have provided the confident three points to extrapolate a likely tunnel trace across the wash (Figure 40). Noise on line 9 prohibited the identification and eventual enhancement of scatter events in this critical portion of the survey area.

For the Otay Mesa POE site we have identified three candidate anomalies with individual anomaly characteristics consistent with numerical and physical models and conform reasonably well to a straight line tunneling approach from a line-to-line perspective. In priority from most similar to least similar the three possible tunnel traces go from west to east (Figure 30). For the San Ysidro Corona Beer site, the anomaly on line 8 at station 8064 is a strong candidate based on anomaly characteristics and proximity to the warehouse; however, a straight line tunnel approach would place the exit point in the park immediately west of the target trailer court (Figure 40).



RECOMMENDATIONS

At this stage of the project it appears critical to merge all the geophysical data together and come up with a collective interpretation. No single geophysical technique provides a unique answer or solution to any problem or question. Each technique is sensitive to a particular earth property or properties, but there are always many interpretations for each observation. It appears we have one reasonable candidate at the San Ysidro site and two, possibly three, at the Otay Mesa POE site. At the POE site, incorporation of the other geophysical data and as much intelligence as possible will be necessary before selecting a candidate that deserves consideration for further invasive investigations. If invasive confirmation is the next step, enhanced processing and modeling of the specific anomaly to be confirmed could greatly reduce the number of boreholes necessary to confirm or refute these interpretations.

REFERENCES

- Cook, J.C., 1965, Seismic mapping of underground cavities using reflection amplitudes: *Geophysics*, v. 30, p. 527-538.
- Fisher, W., 1971, Detection of abandoned underground coal mines by geophysical methods: USEPA Water Pollution Control Res. Ser., Project 14010EHN, 94 p.
- Glover, R.H., 1959, Techniques used in interpreting seismic data in Kansas: In *Symposium on Geophysics in Kansas*, ed. W.W. Hambleton. Kansas Geological Survey Bulletin 137, p. 225-240.
- Ivanov, J., C.B. Park, R.D. Miller, J. Xia, and R. Overton, 2001, Modal separation before dispersion curve extraction by MASW method: Proceedings of the Symposium on the Application of Geophysics to Engineering and Environmental Problems (SAGEEP 2001), Denver, Colorado, March 4-7.
- Miller, R.D., T.S. Anderson, J.C. Davis, D.W. Steeples, and M.L. Moran, 2001, 3-D characterization of seismic properties at the Smart Weapons Test Range, YPG: Proceedings of the 2001 Military Sensing Symposia Specialty Group on Battlefield Acoustic and Seismic Sensing, Magnetic and Electric Field Sensors, Laurel, MD, October 23, published on CD.
- Miller, R.D., C.B. Park, T.S. Anderson, R.F. Ballard, K. Park, J. Xia, and M.L. Moran, 2002, Wavefield imaging to detect underground facilities: Proceedings of the 2002 Military Sensing Symposia Specialty Group on Battlefield Acoustic and Seismic Sensing, Laurel, MD, September 24-26, published on CD.
- Miller, R.D., C.B. Park, J.M. Ivanov, J. Xia, D.R. Laflen, and C. Gratton, 2000, MASW to investigate anomalous near-surface materials at the Indian Refinery in Lawrenceville, Illinois: Kansas Geological Survey Open-file Report 2000-4.
- Miller, R.D., and D.W. Steeples, 1991, Detecting voids in a 0.6-m coal seam, 7 m deep, using seismic reflection: *Geoexploration*, Elsevier Science Publishers B.V., Amsterdam, The Netherlands, v. 28, p. 109-119.
- Miller, R.D., and J. Xia, 1999, Seismic surveys at Alabama Electric Cooperative's proposed Damascus, Alabama site: Kansas Geological Survey Open-file Report 99-12.
- Miller, R.D., and J. Xia, 2002, Tunnel detection mission JT2727-02 final report: Kansas Geological Survey Open-file Report 2002-11.
- Miller, R.D., J. Xia, and C.B. Park, 1999, MASW to investigate subsidence in the Tampa, Florida area: Kansas Geological Survey Open-file Report 99-33.
- Miller, R.D., J. Xia, C.B. Park, and J.M. Ivanov, 1999, Multichannel analysis of surface waves to map bedrock: *Leading Edge*, v. 18, n. 12, p. 1392-1396.
- Nazarian, S., K.H. Stokoe II, and W.R. Hudson, 1983, Use of spectral analysis of surface waves method for determination of moduli and thicknesses of pavement systems: Transportation Research Record No. 930, p. 38-45.
- Park, C.B., R.D. Miller, and J. Ivanov, 2002, Filtering surface waves: Proceedings of the Symposium on the Application of Geophysics to Engineering and Environmental Problems (SAGEEP 2002), Las Vegas, Nevada, February 10-13, Paper 12SE19, published on CD.

- Park, C.B., R.D. Miller, D.W. Steeples, and R.A. Black, 1996, Swept impact seismic technique (SIST): *Geophysics*, v. 61, p. 1789-1803.
- Park, C.B., R.D. Miller, and J. Xia, 1999, Multichannel analysis of surface waves (MASW): *Geophysics*, v. 64, p. 800-808.
- Rechtien, R.D., R.J. Greenfield, and R.F. Ballard, Jr., 1995, Tunnel signature prediction for a cross-borehole seismic survey: *Geophysics*, v. 60, p. 76-86.
- Schepers, R., 1975, A seismic reflection method for solving engineering problems: *Journal of Geophysics*, v. 41, p. 267-284.
- Steeple, D.W., and R.D. Miller, 1990, Seismic reflection methods applied to engineering, environmental, and groundwater problems: Soc. Explor. Geophys. Investigations in Geophysics no. 5, Stan H. Ward, ed., *Volume 1: Review and Tutorial*, p. 1-30.
- Steeple, D.W., and R.D. Miller, 1998, Tunnel detection by high-resolution seismic methods; *in Proceedings of the Third Technical Symposium on Tunnel Detection: Colorado School of Mines*, p. 45-81.
- Watkins, J.S., R.H. Dodson, and K. Watson, 1967, Seismic detection of near-surface cavities: U.S. Geological Survey, Professional Paper 599-A, 12 p.
- Xia, J., R.D. Miller, and C.B. Park, 2000, Advantages of calculating shear-wave velocity from surface waves with higher modes: [Exp. Abs.]: Soc. Expl. Geophys., p. 1295-1298.
- Xia, J., R.D. Miller, and C.B. Park, 1999, Estimation of near-surface velocity by inversion of Rayleigh waves: *Geophysics*, v. 64, p. 691-700.